The RAGazine

Vol 1
Issue 4

June 2014

Photos: Two views of the 530m long, 30m wide 327 MHz cylindrical radio telescope antenna at Ooty, Tamil Nadu, India. The reflector is composed of parallel stainless steel wires, the whole cylinder being supported on 24 steerable parabolic supports.
Courtesy: Tata Inst. Fund. Res.

www.britastro.org/radio/

British Astronomical Association
Radio Astronomy Group

The RAGazine

The quarterly newsletter of the British Astronomical Association, Radio Astronomy Group (BAA RAG)

Vol 1 Issue 4 June 14

BAA, Burlington House,
Picadilly, London,
W1J 0DU
(+44) 207 734 4145
Reg charity 210769

RAG co-ordinator Paul Hyde
RAGazine editor Dave James

The *RAGazine* is published in primarily electronic form, for download in (usually) low and high resolution .pdf formats at:
http://www.britastro.org/radio/downloads.html
For a free subscription to *RAGazine,* send an empty e-mail request with 'subscribe' as the header to:
baa-rag-subscribe@yahoogroups.com

Publication is now around the first day of Aug, Oct, Dec, Feb, Apr and June. Baa-rag Yahoo! subscribers receive an e-mail alert containing the download links when each new issue is available. A few paper copies may be made available on request. We solicit items of news; articles on construction and observing projects; on outreach and educational areas; book reviews; historical descriptions; anecdotes etc. - anything of potential interest to amateurs in radio astronomy and geophysics. We also encourage inclusion of relevant individual and commercial adverts, for sale and wanted, and volunteer appeals (all at no charge). The deadline for contributions is nominally the 15th of the month before the publication date. Contact :

dave@greenover.net

01769 561 002 / 07527 906 346

Most common file and picture formats are acceptable; where possible please contact the editor with advance notice of any contribution. The intended print/view size is A4.

Contents

Editor's Remarks

View from the kitchen

First, I should like to apologise for the week's delay in the publishing of this fourth edition, due to personal and family reasons beyond my control - or pre-planning. Also as a result of these distractions and the more limited time available, this issue is probably more ragged and with more typos than usual, and in several cases I have had to hold back material to the next issue. Several regular features are also missing; alas, we are humour-less, for instance. Sorry to all readers, and especially to those authors with contributions I had intended to include in this issue.

Nevertheless, I hope you like this fourth issue which again has some tasty gems for all - neophyte through seasoned enthusiast, I think. It includes, for example, a reprint of the seminal publication by Reber in 1940, following the similar Jansky one in the last issue.

It's been a busy first year, and *RAGazine* would definitely seem to fulfil a need for the radio astronomy and geophysics amateur community. So now perhaps the good news. As explained in the last issue, we will now move from a quarterly issue interval to a bimonthly basis (every other month, not each fortnight !), probably with a slightly smaller page count. I am also moving the (nominal !) deadline for material submissions to a more easily remembered 15th of the month before that of the cover date, which latter will still be around the first day of the month. So here is the new schedule:

Aug. issue	appears first day of Aug.	15th July is deadline for inputs
Oct.	Oct.	Sep.
Dec.	Dec.	Nov.
Feb.	Feb.	Jan.
Apr.	Apr.	Mar.
Jun.	Jun.	May

This is, of course, something of an experiment, so if this proves a little over-ambitious we shall have to revert to the quarterly frequency. So if you want lots of interesting radio astronomy and geophysics material to read, you must <u>not</u> leave the work to just a few contributors but make a resolution to contribute something yourself ! This need not be an item on construction or observation, for example; there is lots of scope for other possible input (news, opinion, ideas, humour …..). Remember this magazine is for YOU, the reader - neophyte, expert and all shades between and beyond.

Again, I am also keen to feature members' home observatories, their outreach activities, co-operative ventures and the like. So please consider this, or at least point me in the right direction, as it's not possible for me to easily discern what all are doing or have accomplished. Oh yes, and look out for relevant excitement in imminent issues of BBC's *Sky at Night* magazine …..

Best wishes

Dave James **Editor**

dave@greenover.net

01769 561 002

07527 906 346

Coordinator's Remarks

View from the top

RAG2014 proved to be another successful General Meeting, with over 100 people travelling to the NSC in Leicester to hear a range of talks on radio astronomy topics and amateur activities. A full report of the day will be in a future edition of *RAGazine*. This maintained the tradition of RAG meetings being amongst the best attended of any BAA Section (or Group), showing the level of interest in the subject. Looking down the list of attendees' locations I see Barnstaple, Bournemouth, Bristol, Co. Antrim, Devizes, Kelso, Monmouth and Redruth, showing the distances that many were prepared to travel for the event.

As usual, we had a strong contingent of radio amateurs in both the audience and speaker line-up, with one of our keynote speakers, Prof Paul Cannon, adding his name to the list. This is not surprising given the strong interest in experimentation in the amateur radio community, but it shows that amateur radio astronomy is not the preserve of the BAA.

It was also encouraging to hear about plans from individuals and local astronomical societies for tackling radio astronomy targets. One of the main handicaps for traditional astronomers wanting to branch into radio astronomy is a lack of practical experience. An example is in meteor scatter, where the hardware requirements are not demanding - until you come to fitting the connector onto the end of the coaxial cable. Encouraging cooperation between local radio amateurs and amateur astronomers would help overcome such hurdles and Chris Jackson (M6CXJ, President of Nottingham AS) and Victoria Penrice (M6VXJ, NAS Secretary) are currently establishing a list of regional contacts for this. They have RSGB backing for this and I hope that it will lead to even greater participation by the radio amateur community. Further details are included elsewhere in this issue of *RAGazine,* and if you or any other local astronomers or radio amateurs would like to get more involved with radio astronomy, please get in touch with them.

Looking to the future, I would like to see amateur RA events held right across the country, but we do need support in finding venues and organising at the local level. If you feel that there would be interest in a Radio Astronomy meeting in your area and are prepared to help out, please let me know.

This fourth edition of *RAGazine* marks the completion of its first year and once again I'd like to thank Dave James for taking on the Editor's role. Thanks also to those who have contributed material, the lifeblood of any periodical. Please keep it coming so that we can give Dave the headache of deciding which articles will have to be deferred to the next edition. Please also note the change next issue to a more frequent, bimonthly issue cycle as described on the previous page.

Best wishes

Paul Hyde **BAA RAG Coordinator** g4csd@yahoo.co.uk

Radio Astronomy Interest Group (RAIG)

News: RAIG, not RAG

Recently members of Nottingham Astronomical Society (NAS) have initiated the formation of RAIG, which is planned to operate nationally and aims to foster the growth of regional practical amateur astronomy groups. The idea is develop co-operation with organisations such as the RSGB, BAA RAG, universities, academic bodies and institutions who have extant or potential interest or involvement in radio astronomy (and geophysics, one assumes).

The RSGB and BAA RAG's Co-ordinator have already indicated support for this initiative, and RAIG plans to act as a catalyst for the encouragement of regional interest groups, the collaborative preparation of useful support materials, of fostering joint projects and so on.

They key contacts are as follows:

Chris (M6CXI)	president@nottinghamastro.org.uk	07415 094 820
Victoria (M6VXU)	secretary@nottinghamastro.org.uk	

RAIG is currently conducting a survey to gauge the level of interest in amateur RA across the country, in particular seeking inputs from amateur astronomy and radio societies, individuals and others. Key individuals from the relevant professional communities are also to be identified. We will bring more detailed news in a forthcoming *RAGazine* issue.

If you are interested and/or could assist, please contact RAIG.

VLF Quarterly Observing Report, to End May 2014

- John Cook jacook@jacook.plus.com

Observing, VLF

Fig 1 shows activity levels since 2005. The relative sunspot number is a weighted 13 month average, and so values over the last six months are provisional. Sunspot data is courtesy of the BAA Solar Section. SID figures for the last three months are:

2014 February = 88,
2014 March = 85,
2014 April = 67.

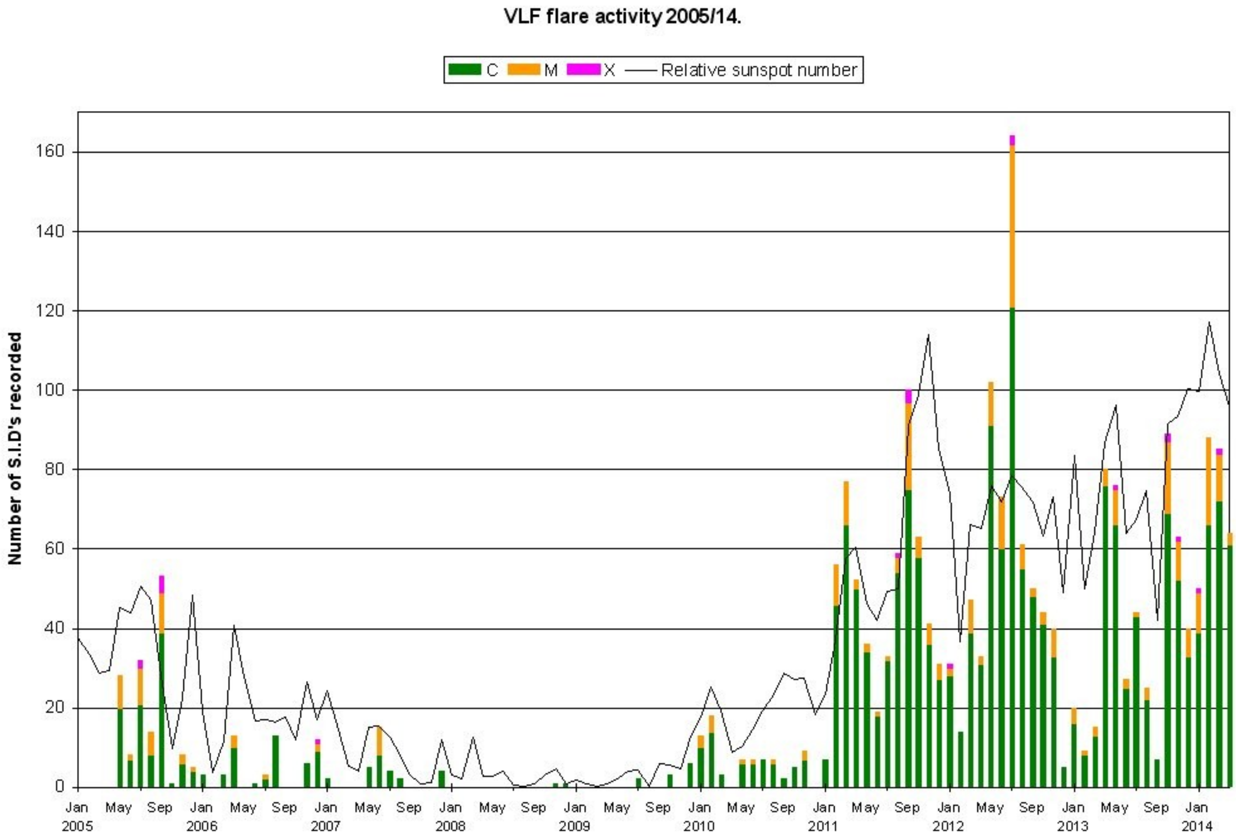

Fig 1 Activity chart

February and March are both well up on the last three month period, although still only half of the 165 SIDs recorded in 2012 July. April is down a little, although the SID count is also provisional as I do not have all of the reports to hand yet. There was a single X-class flare recorded in the early evening of March 29th. This shows in the recording by Roberto Battaiola (Fig 2) from Milan, disrupting the normal sunset effect.

A rather unusual triple-peaked SID was widely recorded on February 2nd. Fig 3 shows the recording by Mark Edwards in Coventry. The first peak is listed by SWPC as X-ray class M1.3, and was caused by active region AR1967. The second peak is listed as C7.8 from AR1968. The third peak is not listed by SWPC, and is presumably a continuation of either of the first two flares.

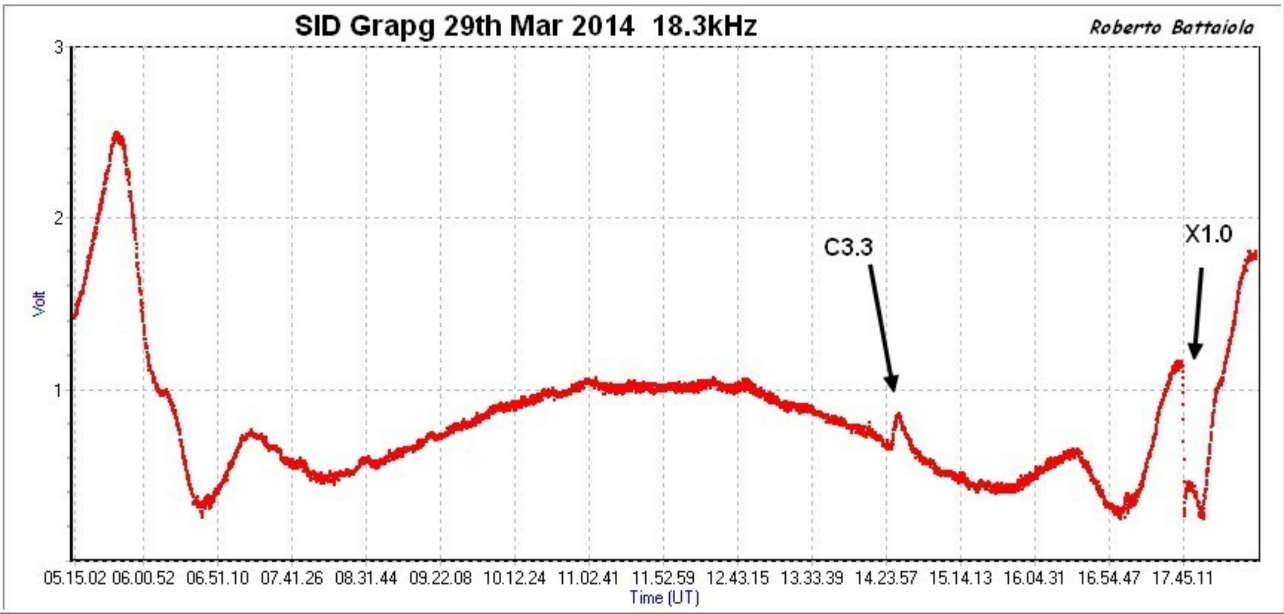

Fig 2: March 29th. Roberto Batttaiola, Milan

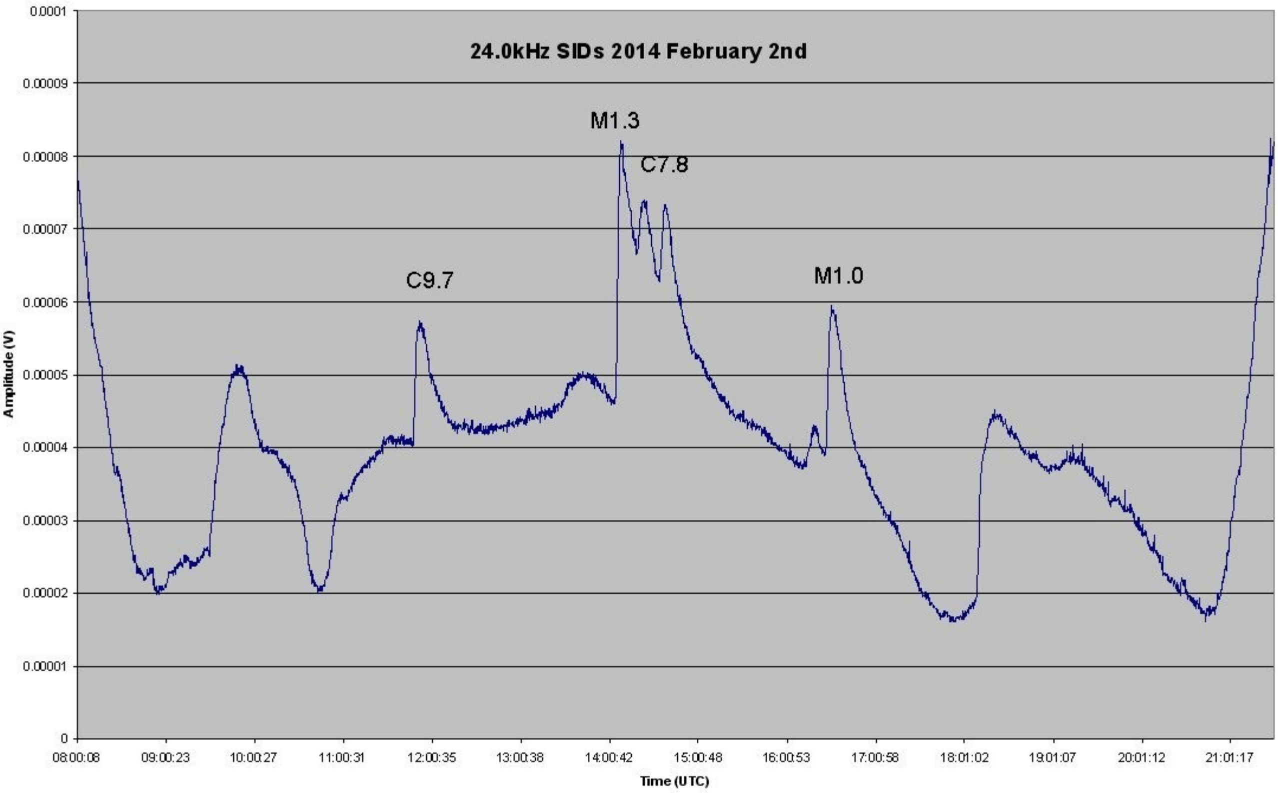

Fig 3: February 2nd. Mark Edwards, Coventry

A rather unusual triple-peaked SID was widely recorded on February 2nd. Fig 3 shows the recording by Mark Edwards in Coventry. The first peak is listed by SWPC as X-ray class M1.3, and was caused by active region AR1967. The second peak is listed as C7.8 from AR1968. The third peak is not listed by SWPC, and is presumably a continuation of either of the first two flares.

There was also a strong X4.9 flare at 00:49UT on February 25th. Although far too early in the morning to be recorded as a SID, it had a strong associated CME that we recorded arriving at 16:53UT on the 27th. Using the SWPC timing of the flare gives a CME transit time of 64 hours 4 minutes. This gave rise to a widespread Aurora over the UK, visible to those lucky enough to have a good dark sky. There are some superb images from this display on the BAA website gallery pages. The magnetic disturbance continued until about 03UT on the 28th. An M3.0 flare on February 20th also produced a CME. This produced a two hour magnetic disturbance starting about 18:00 on the 23rd, well recorded by Colin Clements in Lisburn (Fig 4).

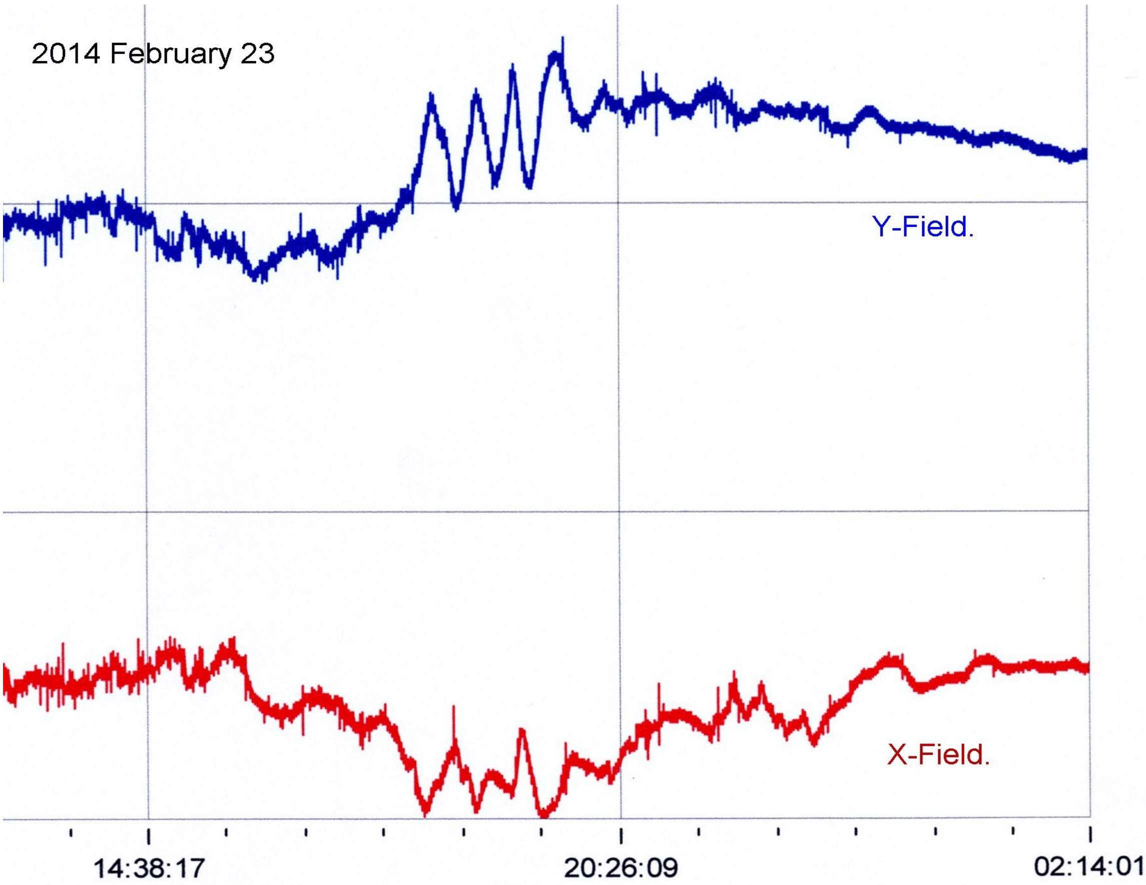

Fig 4: February 23rd. Colin Clements, Lisburn

The orbit of the satellite (GOES15) recording solar X-ray flux has a seasonal period of eclipses such that it is unable to see the sun for up to an hour each day. Most days during March included an eclipse period around 09UT, making life difficult when allocating X-ray flares to our recorded SIDs. I have included these SIDs in the statistics as C-class flares, totalling seven in March.

Fig 5 shows SIDs recorded by Paul Hyde on March 11th. The peak marked 'E' occurred during an eclipse period, but is quite well defined at 23.4kHz (yellow) and 22.1kHz (blue). The C6.7 flare occurred after the eclipse period, showing at all three frequencies. The small SID marked '?' is not listed by SWPC although it does show in the GOES X-ray data. The M1.7 flare makes a big impact at all three frequencies. The following four show best at 22.1kHz, including two more not listed by SWPC, but present in the GOES data. Lists of solar flares can be found in the weekly bulletins produced by the SWPC www.swpc.noaa.gov/weekly. Daily GOES data can also be found at the same website.

Despite the high SID count in March, magnetic activity was rather subdued. An M1.7 flare at 15:24UT on the 10th produced a very small SFE, measured at just –3nT by my magnetometer. Most CMEs seem to have been from near the solar limb, and so directed away from Earth.

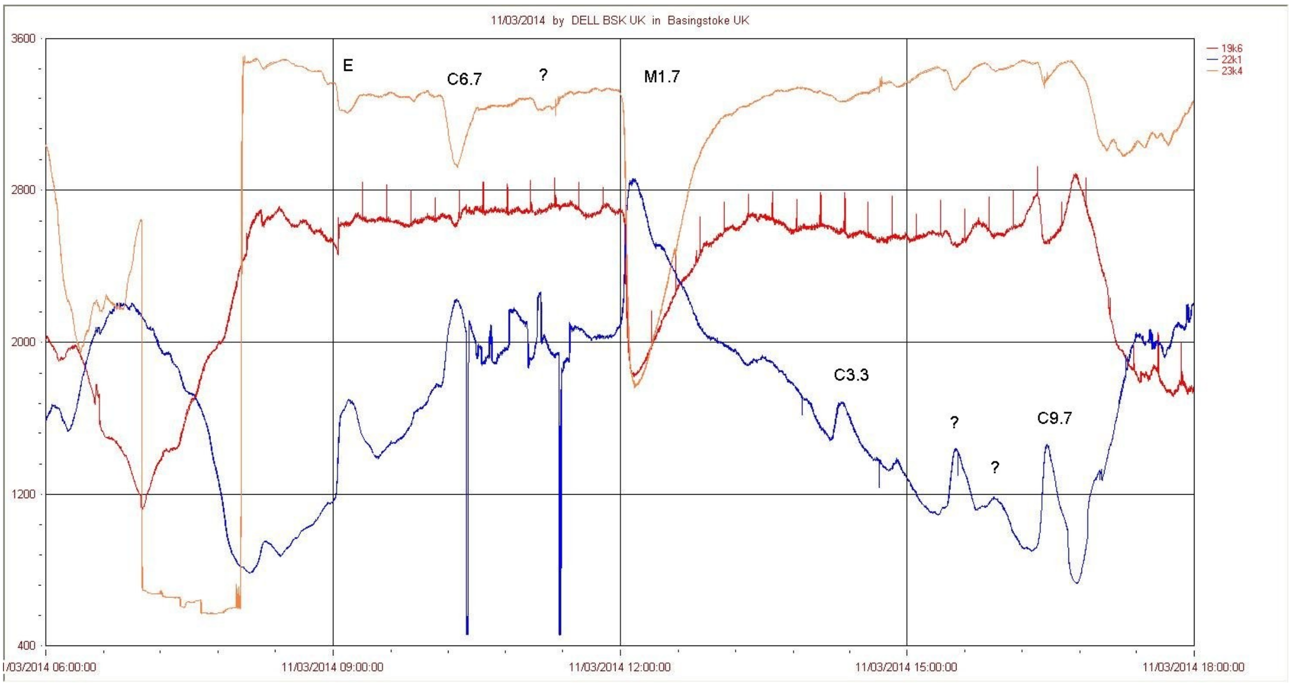

Fig 5: March 11th. Paul Hyde, Basingstoke

The SID count for April was lower than previous months, with many flares being less energetic. Included in the total were three B-class flares recorded as rather small SIDs. Often lost in the clutter from larger events, a very quiet period at the end of April produced B6.0, B7.3 and B9.7 flares that we recorded as SIDs. My own recording from April 29th is shown in Fig 6. Although there were a number of complex active regions present at the time, this B9.7 flare was from AR2048, a small decaying group approaching the western limb of the Sun.

Magnetic activity in April was again rather low. The most active period recorded began around 23UT on the 11th and lasted through most of the 12th. This was caused by the solar wind driving the Bz component of the Sun's magnetic field in a southward direction, thus increasing its coupling with the Earth's field.

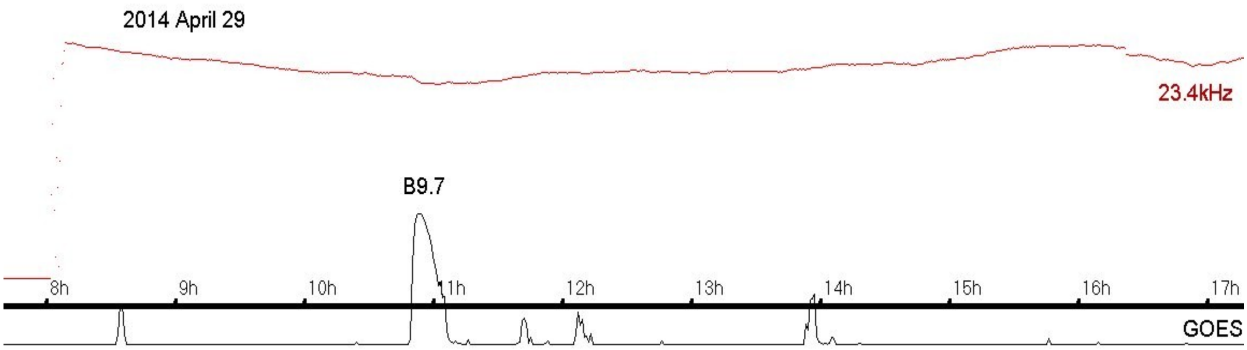

Fig 6: April 29th. John Cook, Wolverhampton

Observers: Roberto Battaiola, Roger Blackwell, Colin Clements, Mark Edwards, John Elliott, Gordon Fiander, Paul Hyde, Richard Kaye, Bob Middlefell, Steve Parkinson, John Wardle, Gonzalo Vargas, John Cook.

My thanks to all contributors.

If you would like to add your own observations, please contact jacook@jacook.plus.com.

Fig 7 Bartels chart
/ see over /

[Editor's note: The brief appendix following the Bartels chart, explaining some of the abbreviations used in these reports and introduced for the first time last issue, has been reproduced again here. Future reports will be bimonthly]

ROTATION | KEY: | DISTURBED. | ACTIVE | SFE | B, C, M, X = FLARE MAGNITUDE. | Synodic rotation start (carrington's).

2423 F	24 MCC	25 C	26 C	27	28 MC	2011 March 1 CCC	2 C	3 CC	4 C	5 CCCC	6 CCCC	7 CMMM	8 CMM	9 CMMM	10 CCCC	11 CCC	12 BCCC	13 CC	14 CBCM	15 CCCC	2108 16 CC	17	18	19	20	21 CC	22 C
2424 F	23 BC	24 MCB	25 C	26	27	28 C	29 C	30	31	2011 April 1	2	3	4	5	6 CC	7 C	8	9 C	10	11 BC	2109 12 C	13 CCCC	14 CCCC	15 CCCM	16 CBCC	17 CB	18 B
2425 F	19 B	20 BBC	21 CCC	22 CCMCC	23 CC	24	25 B	26	27	28 CCCC	29	30 CCCC	2011 May 1 CB	2 C	3 C	4	5	6	7	8	2110 9 C	10	11	12 C	13	14	15 C
2426 F	16	17	18 CCC	19	20	21	22	23	24	25	26	27 BCCC	28 CCCM	29 CBCM	30 CCC	31	2011 June 1	2	3	4	5	2111 6	7	8	9	10	11
2427 F	12	13	14	15	16	17	18	19	20	21	22	23	24	25	26	27	28	29	30	2011 July 1	2	2112 3 C	4	5	6	7	8 CCCC
2428 F	9	10	11 C	12 C	13	14	15	16	17	18 C	19	20	21	22	23	24	25	26	27 CCCM	28 CCBCC	29 CCCB	2113 30 CCCC	31 CBCC	2011 August 1 CCCC	2 MCCB	3 MCCM	4 CCCC
2429 F	5 CCCB	6 CCCC	7 CCC	8 CMC	9 CMXC	10 CCCC	11 CC	12	13	14	15 CB	16	17 CC	18 BC	19	20 BB	21 BC	22 C	23	24 C	25 BC	26 C	2114 27	28	29 CCC	30 CBC	31 C
2430 F	2011 September 1 CCC	2 C	3 CCCC	4 CMCC	5 M	6	7 X	8 CMC	9 C	10 MC	11 CCB	12 C	13 C	14 CCCC	15 CCC	16 CCCC	17 CC	18 CCC	19 CC	20 CCCC	21 CMCC	22 CMXC	2115 23 CCCC	24 CXMM	25 MMCM	26 CCMC	27 CCCC
2431 F	28 CCM	29 CC	30 M	2011 October 1 MC	2 CCMC	3	4 C	5 CCCB	6 C	7	8	9 C	10 CCC	11	12 CCCC	13 CCC	14 CCC	15 CCCC	16 CCCC	17 CC	18	19 CC	2116 20 C	21 CMC	22 MC	23 C	24
2432 F	25	26 C	27	28 C	29 CCCC	30 CCC	31 M	2011 November 1 C	2 CCCC	3 CCM	4 C	5 CMCC	6 CC	7	8	9 M	10	11 C	12 C	13 CC	14 CCC	15 MM	16 C	2117 17 CCC	18	19	20 CCCC
2433 F	21	22 C	23 C	24	25	26	27 C	28 C	29 C	30	2011 December 1 C	2	3	4	5 C	6	7	8	9 C	10	11	12 B	13 C	2118 14 CCC	15	16	17
2434 F	18 B	19	20 C	21 CCCC	22	23 C	24	25 CCM	26 CC	27 C	28 CCC	29 M	30 CCC	31 MBM	2012 January 1	2 C	3	4 CC	5 C	6 C	7	8 CC	9 CC	2119 10	11 C	12 CC	13
2435 F	14 CMC	15 C	16 CC	17	18 CC	19 CM	20	21 C	22 CC	23	24 C	25	26 C	27 CCX	28 C	29	30	31	2012 February 1	2	3	4	5	6	2120 7 C	8	9 C
2436 F	10 CC	11 CCCC	12 C	13	14	15	16	17	18	19 C	20 C	21 C	22	23	24	25	26 C	27	28	29	2012 March 1 C	2 M	3	4 MC	2121 5 CCCC	6 MCMC	7
2437 F	8 C	9 CC	10 CCM	11	12 C	13 M	14 M	15 MC	16 CC	17	18	19 C	20	21 BCCC	22 CCC	23 C	24 C	25	26	27	28	29 CCCC	30	31	2012 April 1	2	3
2438 F	4 C	5 BC	6	7 C	8	9 C	10 B	11	12	13	14	15	16 M	17	18 CCBCC	19 C	20 CCC	21 CB	22 CC	23 C	24 CC	25 C	26	27 MCC	2123 28 C	29 CC	30 CCCC
2439 F	2012 May 1	2 CBCC	3 CC	4 CC	5 CCMCC	6 MCMC	7 CCMC	8 CCMC	9 CBMM	10 MCCC	11 CCCC	12 CCCC	13 CC	14 CCCC	15 CBC	16 CC	17 M	18 CCCC	19 C	20	21	22	23	24 CBBC	25 CC	2124 26 CC	27
2440 F	28 BB	29	30 C	31 CCCC	2012 June 1 C	2	3 C	4 M	5 CC	6 CCM	7 CCCC	8 CCMCM	9 CMCMC	10 M	11 CCCC	12 CCCC	13 CMCC	14 CCCM	15 CC	16 C	17 CC	18	19 CC	20 CC	21	2125 22	23
2441 F	24	25	26 C	27 CCCC	28 CMC	29 CCMC	30 CCMCM	2012 July 1 CCCM	2 CMCM	3 CCCC	4 MMMM	5 MMMM	6 MMMX	7 MMMC	8 MMMM	9 CCCC	10 MMCC	11 CCCC	12 CX	13 CCCC	14 MCCC	15 C	16 CCC	17 M	18 C	2126 19 M	20
2442 F	21	22	23 CB	24 CCCC	25	26 C	27 CCCM	28 CCM	29 MCC	30 CCCM	31 CCCC	2012 August 1 CCCC	2 C	3 CCC	4 C	5	6 CCCC	7 CCCC	8 CCCC	9 CCC	10 CC	11 MC	12	13 CCC	14 C	2127 15	16 C
2443 F	17 CMCM	18 MCCM	19	20	21	22	23	24	25	26	27	28	29 C	30 CCM	31 CCCC	2012 September 1 CCC	2 CCC	3 CCC	4 C	5 CCC	6 MCCC	7 C	8 M	9 CC	10 CCC	11 CB	2128 12 CC
2444 F	13 CCC	14	15	16	17 CCC	18 CC	19 CC	20	21	22	23	24 C	25 CC	26	27 C	28	29 CCCC	30 CCC	2012 October 1 CCCC	2 C	3	4	5	6	7	8 CCMC	2129 9 CCCC
2445 F	10 CMBC	11 CCC	12 CB	13 B	14	15	16 C	17 CCCC	18	19	20 CM	21 CCC	22 C	23 CCC	24 CCCC	25	26 CC	27	28	29	30	31 C	2012 November 1	2	3	4	2130 5 B
2446 F	6	7	8	9	10 C	11	12 CC	13 CMMC	14 CMC	15 CCCC	16 C	17	18 CC	19	20 CCMC	21 MCM	22	23 C	24 C	25	26 CCC	27 CCCM	28 C	29 CC	30 C	2012 December 1 CC	2
2447 F	2131 3	4	5	6	7	8	9	10	11	12 C	13	14 C	15	16	17	18	19	20	21	22	23	24	25 C	26	27	28	29
2448 F	2132 30	31	2013 January 1	2	3	4	5 MC	6 CC	7 C	8	9 CC	10 CC	11 MM	12 MCCC	13	14 C	15 C	16	17	18 CC	19	20 C	21	22	23	24	25
2449 F	2133 26	27	28	29	30	31	2013 February 1	2	3	4	5 C	6	7	8	9	10	11	12	13	14	15	16	17 CM	18	19 C	20 CC	21 B
2450 F	2134 22 C	23 C	24 C	25	26	27	28	2013 March 1	2 C	3	4	5 M	6	7 C	8	9	10	11	12 CC	13 C	14	15 MC	16	17 C	18 C	19 CC	20
2451 F	2135 21 C	22 CBC	23	24	25	26	27	28	29	30	31	2013 April 1	2 B	3 CBC	4 C	5 M	6 CCC	7 CC	8 C	9 CCCC	10 CCC	11 MCCC	12 CM	13 C	14	15 C	16 CC
2452 F	2136 17	18 C	19 C	20 CC	21 CCCC	22 M	23 CCCC	24 CCCC	25 CCCC	26 CCCC	27 CCCC	28 CCCC	29 CC	30 CCC	2013 May 1 CCCC	2 MC	3 CCMM	4 CCCC	5 CCCM	6	7 CBC	8	9 CCC	10 CMCC	11 CCCC	12 CCC	13 CCMX
2453 F	14 C	2137 15	16 CC	17 M	18 C	19 CCCC	20 CCCM	21	22	23 CCCC	24	25 C	26 C	27	28	29	30	31 M	2013 June 1	2	3 C	4	5 M	6	7 CC	8 C	9
2454 F	10 BC	2138 11	12	13	14	15	16	17	18	19 CC	20 CCC	21 CC	22 C	23 M	24 CCCC	25 B	26 C	27 CBC	28 C	29	30 CCCC	2013 July 1 CC	2 CC	3 MCCC	4 CCCC	5 CCCC	6
2455 F	7 CB	2139 8	9 C	10 C	11 CC	12 C	13 C	14 C	15 CC	16 C	17 C	18 CC	19	20	21 CC	22	23	24	25	26	27 C	28 CCCC	29 C	30	31	2013 August 1	2
2456 F	3	2140 4	5	6	7	8	9	10	11 CCC	12 M	13 CCCC	14 CCC	15 CC	16 CC	17 CMM	18 C	19 C	20 C	21 CC	22 C	23	24	25	26	27	28	29
2457 F	30	31 C	2013 September 1 C	2	3 BC	4 C	5	6	7	8	9	10	11	12	13	14	15	16	17	18	19	20 CCCC	21	22	23	24	25
2458 F	26	27	2142 28	29	30	2013 October 1	2	3	4	5	6 C	7 C	8	9 C	10 CCCC	11 MCCC	12 CCC	13 C	14 C	15 CMCC	16 CCC	17 CCM	18 CCCC	19 CCC	20 CC	21	22 CCCM
2459 F	23 CCCC	24 CMMC	2143 25 XMXM	26 MMMM	27 CCMC	28 MMMM	29 CCCC	30 C	31 MCC	2013 November 1 C	2 CCC	3 C	4 CCC	5 MCCM	6 CCCM	7 CCMC	8 M	9 CC	10 CCC	11 CMC	12 CC	13 CCCM	14 CCC	15 C	16 MCC	17 CCC	18 CCC
2460 F	19 X	20 CC	2144 21 M	22 C	23 CCM	24 CC	25	26	27	28	29	30	2013 December 1 C	2 C	3	4	5 C	6 C	7	8 C	9 CCC	10	11 CC	12 C	13	14 CC	15 CC
2461 F	16 C	17	18	2145 19 C	20 CMCC	21 C	22 MMMM	23 M	24	25 C	26	27 CC	28 CC	29 MCCC	30 C	31 C	2014 January 1 C	2 C	3 CCMC	4 CCMC	5 C	6 C	7 CMCX	8 CCCC	9	10	11 CCC
2462 F	12	13 CC	14 C	2146 15	16 C	17 CCCC	18 CC	19	20	21	22	23	24	25	26 C	27 C	28 MMMM	29 CCC	30 MCC	31 CM	2014 February 1 CCCC	2 MMMM	3 CCCC	4 MCCM	5 CCCM	6 CCC	7 CCMC
2463 F	8 CCC	9 M	10 CC	11 CM	2147 12 CM	13 MCCM	14 CMMM	15	16 MCC	17 CCC	18 CC	19 C	20 M	21 CC	22 C	23 CC	24 MMC	25 C	26 CCM	27 CCCC	28 CCC	2014 March 1 MC	2 CCC	3 CCCM	4 CCCC	5 C	6
2464 F	7	8	9 CCMM	10 CCCM	2148 11 CMCC	12 CMC	13 CCM	14 C	15 CCC	16 CC	17 CCC	18 C	19 CCCC	20 CC	21 C	22 MCC	23 CC	24 CC	25	26 CC	27	28 CM	29 CCCX	30 M	31 MC	2014 April 1	2 CCM
2465 F	3 CC	4 CCC	5 CCC	6	2149 7 CC	8	9	10 C	11 CCC	12 C	13 C	14 CCCC	15 CCCC	16 CCCM	17 CC	18 CM	19 CCCC	20 CCCC	21 C	22 CCCC	23 CCCC	24 C	25 CC	26 C	27	28 BC	29 B
2466 F	30 B	2014 May 1	2	3	4	2150 5	6	7	8	9	10	11	12	13	14	15	16	17	18	19	20	21	22	23	24	25	26

Appendix: Common Abbreviations

In general it can be very confusing to newcomers, but can also be a useful shorthand when writing. This list should help to explain those used in my summaries of Solar and magnetic activity.

SIDs: Sudden Ionospheric Disturbances.
These are the characteristic effects seen in the Earth's ionosphere in response to solar X-ray flares. They are recorded by monitoring the signal strength of a remote terrestrial transmitter, and take the form of sudden changes in received signal strength. Signals in the VLF (q.v.) spectrum are used, as they are reflected / refracted by the ionosphere's D-region (q.v.) where the X-ray and UV energy has its greatest effect.

SEA: Sudden Enhancement of Atmospherics.
Rather than monitoring a known transmitter to detect solar flares, natural atmospherics from remote lightning storms can be used instead. As with a SID, the D-region disturbance can be recorded as an enhanced reception of these natural VLF radio signals. SEA monitoring was very popular in the early days of BAA radio astronomy.

VLF: Very Low Frequency.
Usually refers to the spectrum between 3kHz and 30kHz. For solar flare monitoring the range in use is usually 15kHz to 40kHz.

D-region:
This is the name given to the lowest part of the Earth's ionosphere at an altitude of about 70km. The level of ionisation present in the D-region (the electron density) is directly controlled by Solar radiation such that its radio wave propagation characteristics can be used to detect changes in Solar activity. Normal daytime radiation from the Sun produces a level of ionisation that varies with the Sun's altitude in the sky through the day. The absence of sunlight at night allows electrons to recombine leaving a neutral charge.

SI: Sudden Impulse.
An abrupt change in the Earth's magnetic field, caused by the arrival of a region of enhanced solar wind velocity or density.

SSC: Storm Sudden Commencement.
A change in the rhythm of the Earth's magnetic field following a Sudden Impulse. This is often followed by a longer lasting magnetic storm.

CME: Coronal Mass Ejection.
The ejection of a part of the Sun's corona following a solar flare. Depending on the geometry of the flare, the CME may or may not be directed towards the Earth. CMEs are usually responsible for the SI/SSC transients recorded in magnetograms. The ejected mass is in the form of charged particles, and so travels through space much more slowly than the electromagnetic radiation from the original flare.

SFE: Solar Flare Effect.
A SFE occurs when a very rapid increase in D-region electron density is produced by the X-ray and UV output of a solar flare. This rapid change in ionisation causes a rapid change in current flow in the D-region, and therefore a rapid change in the magnetic field. On a magnetogram, an SFE occurs at the same time as the flare (or recorded SID), while a SI or SSC will be delayed by a day or more according to the solar wind speed.

nT: Nano Tesla.
The SI unit of magnetic flux density, named after Nicola Tesla.

Advertisements

Advertising

[Advertising feature]

Radio Astronomy Supplies
International Supplier of Research Radio Telescopes Since 1994

PRODUCT NEWS AND DATA SHEET

Why Use a Bandpass Filter?

A **band-pass filter** is a device that passes frequencies within a certain range and rejects (attenuates) frequencies outside that range.

A band-pass filter can be characterized by its Q-factor. The Q-factor is the inverse of the fractional bandwidth. A high-Q filter will have a narrow passband and a low-Q filter will have a wide passband. These are respectively referred to as narrow-band and wide-band filters.

Bandpass Q Response

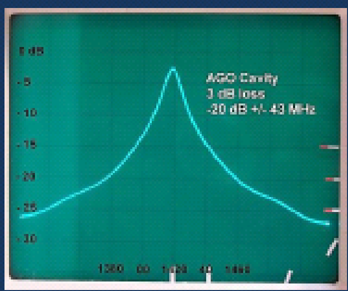

1420 MHz. Bandpass Filter

Radio Astronomy Supplies and WD5AGO, have perfected a superb Bandpass Filter for Radio Astronomy Research.

Developed by our lead LNA Design Engineer, Tommy Henderson, WD5AGO. This filter has replaced the multi-pole filter. The sharp response curve offers a tighter defense against any RFI that would interfere with observations in the Continuum and Spectral modes.

SPECIFICATIONS

Receiving Frequency	1420.405 MHz (21cm)
Loss	3 dB
Bandpass and Rejection	-20dB @ +/- 43 MHz.

"Custom Frequencies Available on Request"

For additional information, please contact us.
jeff@radioastronomysupplies.com
954 554-3739

Radio Astronomy Supplies
P.O. Box 1097, Whitesboro, Texas 76273

http://www.radioastronomysupplies.com

What's On

Diary

June	27-29	2014	Ham Radio Fest, Friedricshafen, Germany
June	29– 2 July	2014	SARA Annual Conf., Green Bank, WV: see SARA web site*
July	2-3	2014	Radio JOVE Conf., Green Bank, WV: see above
July	25-27	2014	AMSAT Colloquium, Guildford
Aug	23-27	2014	EME 2014, Pleumeur Bodou, near Lannion, France
Sep	6-7	2014	Europ. Conf on Amateur RA, Bad Münstereifel-Eschweiler, Germany
Sep	26-27	2014	National Hamfest (UK), Lincoln
Oct	10-12	2014	RSGB Convention, Milton Keynes

* Star Quest (optical) immediately precedes, 25-29 June at same location, NRAO.

An Introduction to Radio Objects that can be detected by amateur radio astronomers: Part 1 (of 3)

- **David Morgan**   www.dmradas.co.uk

RA Basics

4 Jupiter

4.1 Detection of Jupiter signals

From Figure 2.1 we can see that the signal levels on Earth from Jupiter are about 10^5 Jy which is comparable to the quiet Sun and low level solar storms. The same equipment used to detect solar emissions can be used to receive signals from Jupiter. Greater attention has to be paid the design and positioning of a suitable HF antenna that has some directionality [3, 4]. A wire dipole 22 feet long set between 0.25 and 0.5 wavelengths above the ground will produce a beam at 21MHz such as is shown in Figure 4.1. If this antenna is connected to a communications receiver when Jupiter is positioned to be in the beam a variety of noisy signals may be heard. These vary considerably and are related to the position of the moon Io. There are many web-sites dedicated to observations of the complex emissions from Jupiter [5,6,7] and one should look at these for details of emission classifications and technical details of equipment.

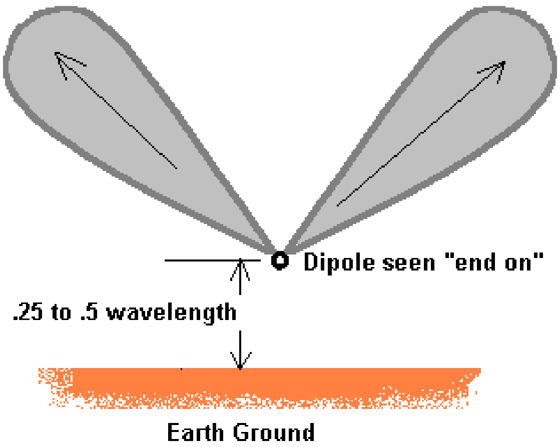

Figure 4.1 Dipole antenna pattern for detection of Jupiter noise

There are three major factors not related to observing conditions on Earth which have been identified to affect the probability of hearing Jupiter's decametric emissions at any given time [8] :

- The central meridian longitude of Jupiter that faces us.
- The position of the innermost moon Io in its orbit around Jupiter
- The Jovicentric declination of the Earth

An illustration of the Jovian radiation belts and the spiral motion of trapped electrons is given in Figure 4.2.

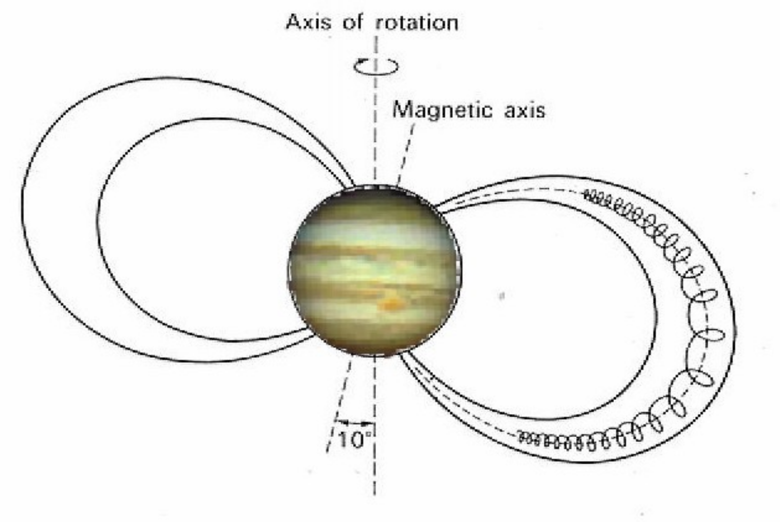

Figure 4.2 Jovian magnetosphere

Some patience is required to detect the radio emissions from Jupiter as conditions are not always favourable and long observing sessions are sometimes needed.

4.2 Spectrum of Jupiter emissions

Signals from Jupiter were first detected in 1958 at a wavelength of ~3cm, but it was not until measurements were made in the HF band that it was realised how strong the emissions were. The spectrum is complex and is composed of two parts as shown in Figure 4.3.

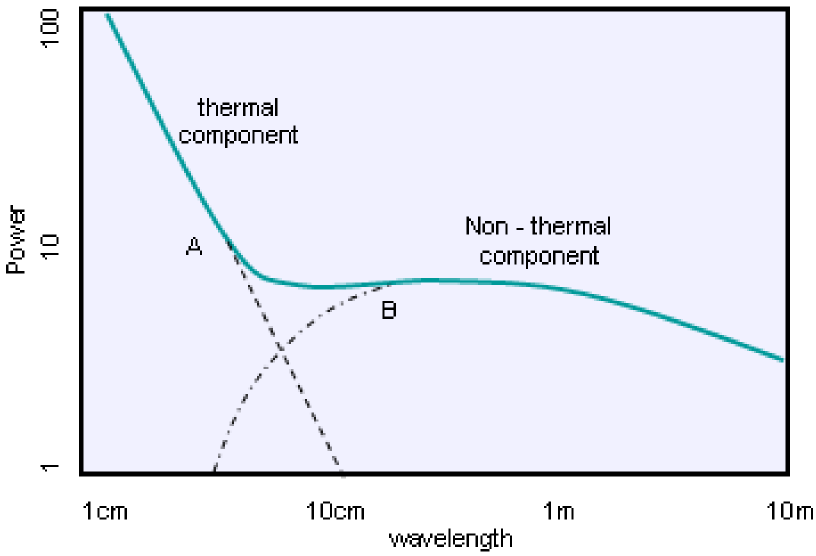

Figure 4.3 Complex spectrum of Jupiter emissions

The thermal component A arises from the cold planet and its atmosphere at a temperature of 130^0 K. The intensity of the non-thermal component B is much greater at wavelengths longer than 10cm and is generated by the interaction of high energy electrons (~10MeV) with the planet's magnetic field that has a strength of about 1 gauss. A centimetric emission map of the active region is shown in Figure 4.4.

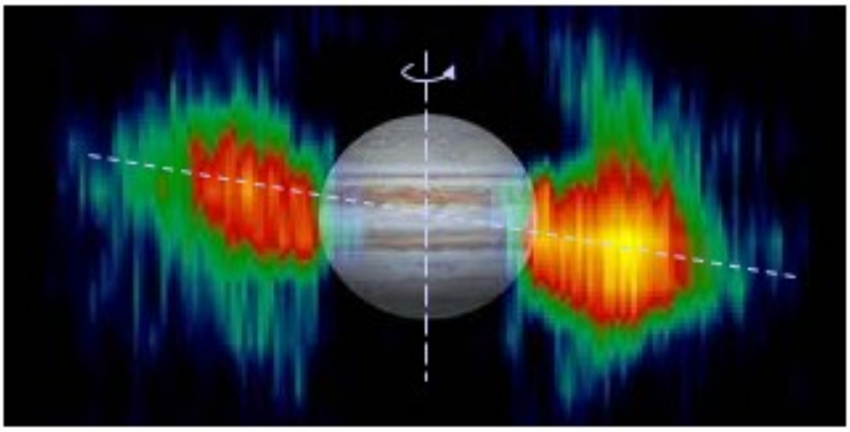

Figure 4.4 Radio emission map at centimetre wavelengths

Jupiter is a good ‘target object’ for the amateur radio astronomer with fairly basic equipment, however a large antenna is required and this can be difficult to erect in a limited space and in the midst of interfering electronic equipment in urban situations.

5 The Moon

The moon is a solid body with no significant atmosphere; it therefore radiates as a cool solid body (thermal radiation) and is not easy to detect at long wavelengths. It is possible for the amateur to make observations with access to an old C band (4 – 8 GHz) satellite TV antenna with a diameter of a few metres as shown in Figure 5.1.

Figure 5.1 3m dish with C band feed

Figure 5.2 The moon

The typical beam width of a 3m diameter dish at 4GHz is ~ 2^0 – rather larger than the angular diameter of the moon at 0.5^0. The moon will therefore present almost a point source to the antenna and a transit scan across the moon will produce a trace with the properties of the antenna beam: ie. a detection that is about 2^0 across. However it is still an interesting exercise to attempt to detect a cold, purely thermal radiating body.

The moon has no significant magnetic field and no ionised gaseous atmosphere containing free electrons, so there is no mechanism to generate non-thermal radio emissions. The thermal signal from the Moon is quite low and a fairly good receiver is needed to make a successful detection.

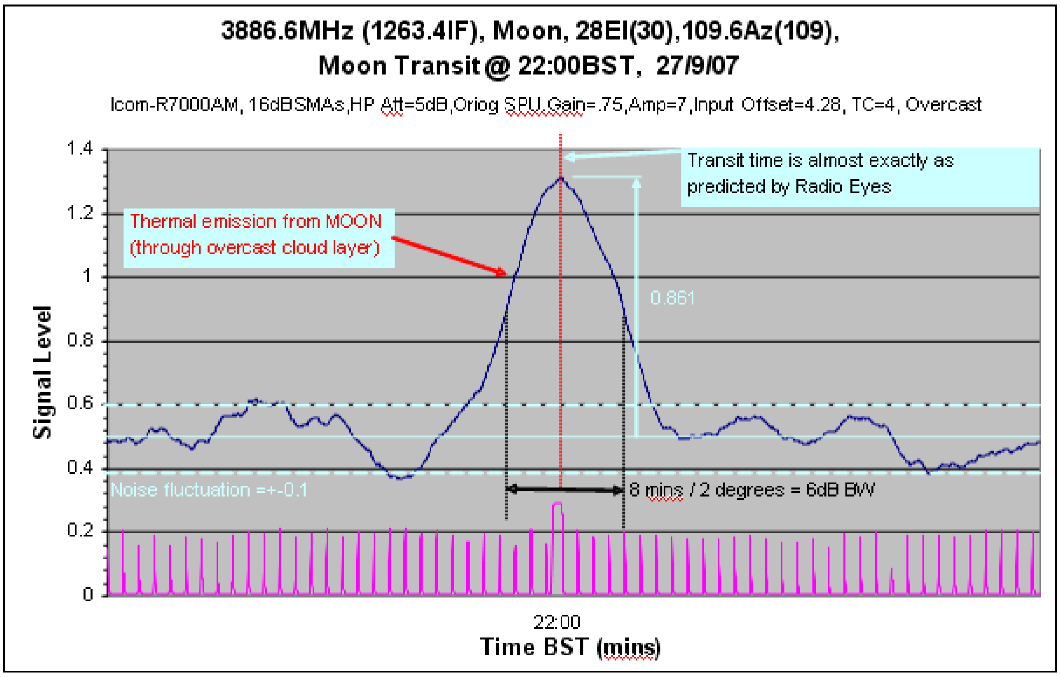

Figure 5.3 Detection of thermal emission from the Moon

6 Galactic Hydrogen Line

6.1 Emissions outside the Solar System

Having examined the emissions from bodies within the solar system, we now look much further out into the Milky Way. The most abundant element in the Universe is Hydrogen and it exists in atomic and ionised forms in large amounts within our galaxy. As discussed in section 2.2.3, atomic hydrogen can emit a specific spectral line at 1420MHz. By measuring the strength of this 'line emission' it is quite possible for the amateur radio astronomer to map the hydrogen distribution in part of our galaxy.

In order to do this, the observer needs good antenna and receiver equipment that is stable over hours and days of observing time. This usually requires the sensitive receiver elements to be temperature controlled to avoid drifts in noise level and receiver gain.

Assuming this can be done, an amateur observer can produce a map such as that shown in Figure 6.1. by measuring the signal strength as a function of transit time at a number of declinations on different days and combining the data with computer software tools.

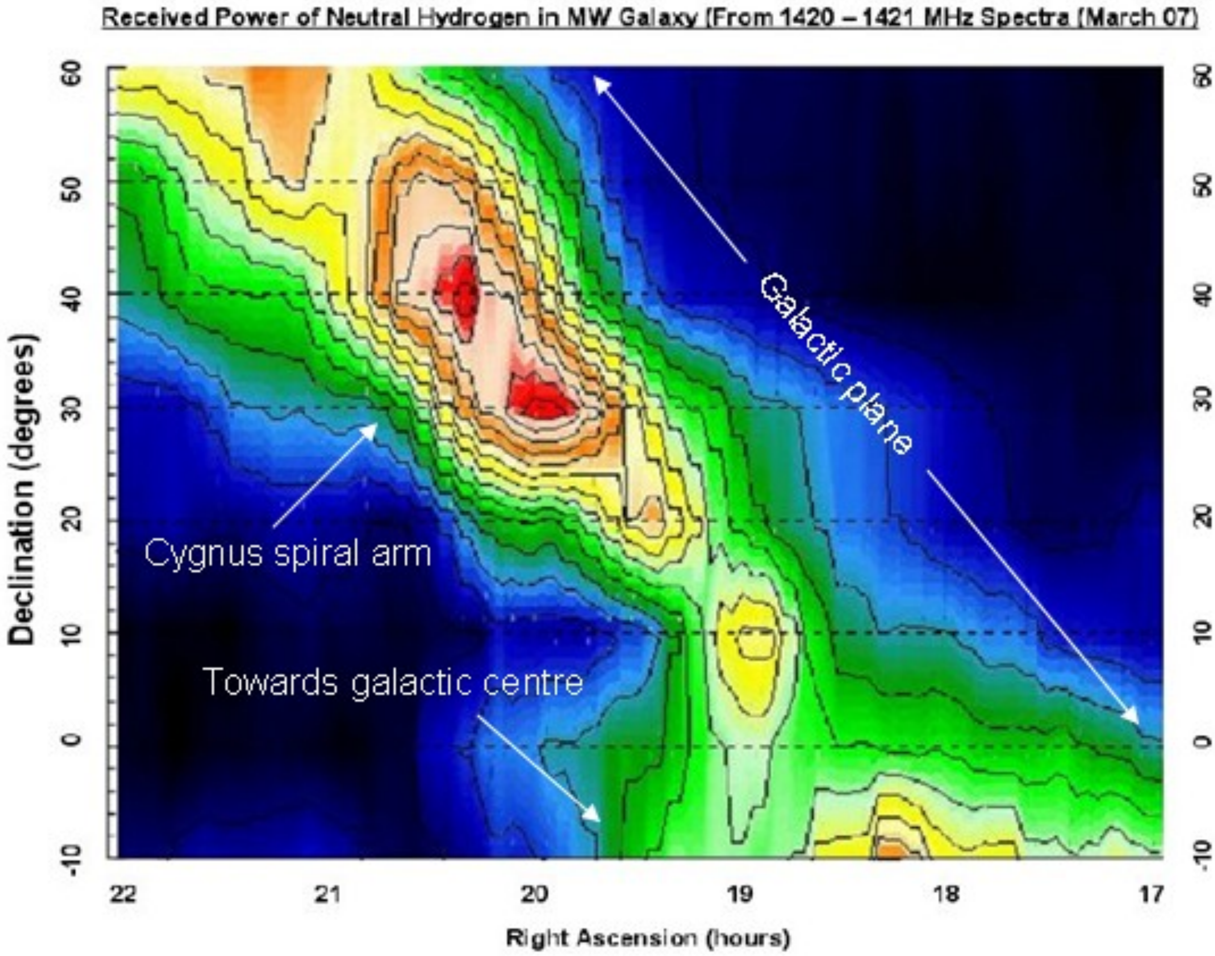

Figure 6.1 Map of atomic Hydrogen in the galactic plane

6.2 Galactic distribution of Hydrogen

The narrow spectral line emission from Hydrogen is Doppler shifted by the relative line-of-sight velocity of the source region to the observer. This provides a way for professional radio astronomers to separate out the signals from different spiral arms of the galaxy, that each have different relative velocities. By this means it is possible to plot the density of Hydrogen (related to signal strength) to the location of the source position (related to the Doppler shift) and generate a 'top down' view of the spiral nature of the galaxy from measurements made from the Earth, which of course lies within the galactic plane.

This cannot be done optically as dust in the galactic plane largely obscures the spiral arms.

In Figure 6.2 we see a 'top down' map of the galaxy produced in 1964. The sector marked in blue is that related to the amateur map in Figure 6.1 The dark sectors along the 0^0 to 180^0 line of galactic longitude is blank because there is insufficient Doppler shift for the calculations to be made.

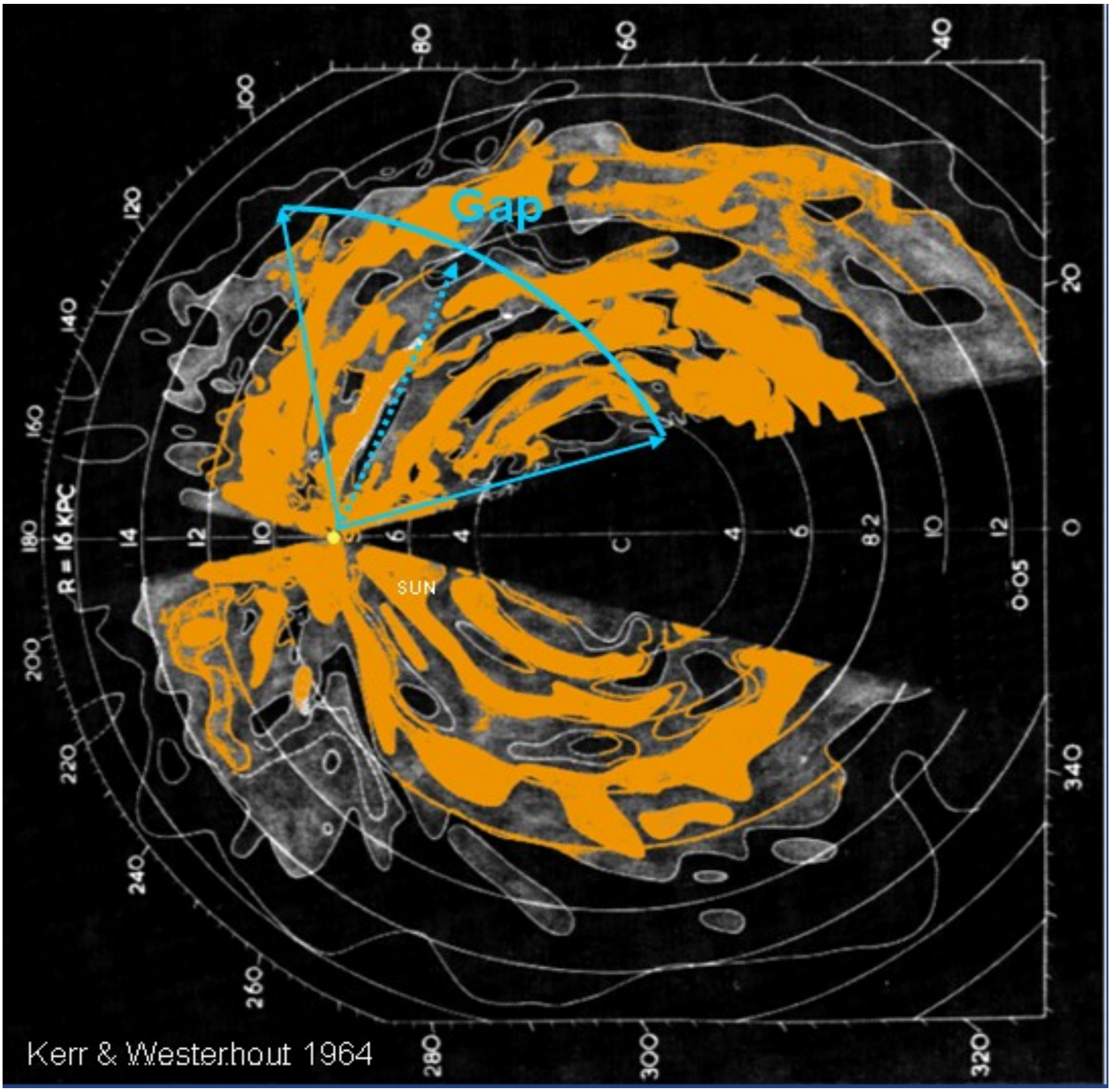

Figure 6.2 Hydrogen distribution in the Milky Way

7 Galactic continuum emissions

7.1 Constituents of continuum emissions

Very broadband continuous radio emissions are referred to as ‘continuum’ emissions and are composed of two main types:

- Thermal emissions
- Cyclotron / synchrotron emissions

The generation mechanisms for both types were discussed in section 2. In this section we look at continuum emissions that can be observed by amateur radio astronomers.

Because of the different spectra, emissions from either type will tend to dominate in certain frequency bands. Thermal emission is more easily detected at high frequencies above a few GHz, whereas synchrotron emission increases with decreasing frequency so is more easily detected at low frequencies in the HF to UHF bands.

It follows that observers should construct equipment that is capable of operation in either frequency regime depending on what type of continuum emission they seek to measure.

7.2 Synchrotron emissions

We will give an example of thermal emission from nebulae later in this paper but here we will examine how the amateur radio astronomer can plot the distribution of synchrotron emission in the Milky Way.

If equipment has been designed to detect the neutral Hydrogen line at 1420MHz it is convenient to use frequencies close to this to observe synchrotron emissions. Because the line emission of Hydrogen is narrow (<1MHz) we can tune the receiver to a frequency close by and detect only the broad band synchrotron signal. In the example that follows, the chosen frequency was 1453MHz – which was far enough away from the Hydrogen line, but still within the bandwidth of the antenna and receiving equipment.

Figure 7.1 3m dish with 1400 -1500MHz feed

By setting the antenna at a series of declinations over a period of several days, a succession of transit scans through the galaxy can be made resulting in a set of plots as shown in Figure 7.2.

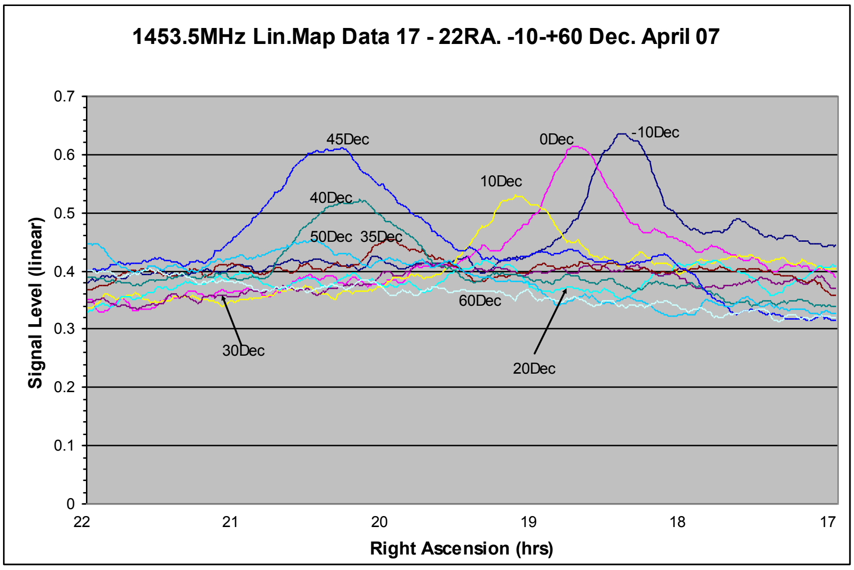

Figure 7.2 Transit scan data (synchrotron emissions)

The data can be assembled as a 'false colour' map using suitable software[9] as shown in Figure 7.3. (next page).

In this diagram we see the radio map at 1453.5MHz converted to galactic coordinates[12] and superimposed on an optical picture of the Milky Way. There are several interesting things to note about this map:

- The low signal level of the emission at galactic longitude of 60^0 corresponds to the gap seen between spiral arms in Figure 6.2. The antenna is pointed in a direction where there is low concentration of matter and plasma and the integrated signal along the line of sight is low. This also shows up on the optical image where the region is largely dark.

- Closer to the centre of the galaxy at a longitude of $\sim 35^0$ there is an excursion on the radio map known as the North Galactic Spur, thought to be part of the giant arc of an ancient supernova remnant. There is no optical counterpart to this feature.

- The radio and optical emissions peak again at a galactic longitude of 80^0 where we are looking along the Cygnus spiral arm and the integrated radio and optical emissions are bright.

As has been shown, detecting the galactic synchrotron emission is a credible project for the amateur radio astronomer.

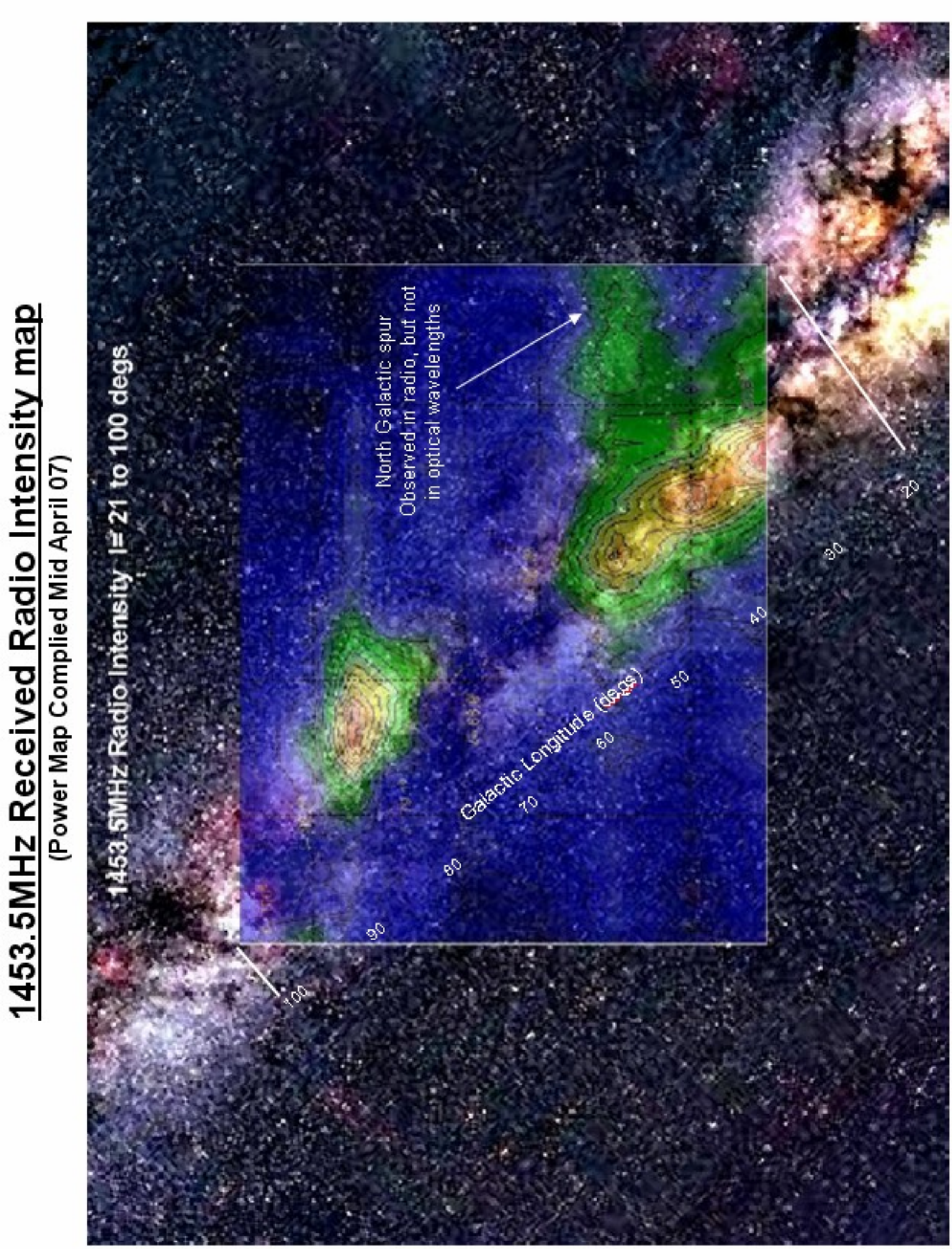

Figure 7.3 Map of galactic radio synchrotron emissions

8 Supernova Remnants

Supernova remnants are vast almost spherical shells of plasma moving with extremely high velocity into space as a result of high mass stellar explosion. The plasma moves – and carries with it – a significant magnetic field with which the plasma interacts to produce strong synchrotron emissions. As the relativistic plasma shock wave slams into the surrounding tenuous interstellar material further emissions are generated.

There are a number of well known supernova remnants in our galaxy, some of which make good observing 'targets' for the amateur radio astronomer.

Name	Light reached Earth	Distance Ly
Cassiopeia A	17th C	10,000
Crab Nebula SN1054	1054 AD	6,300
Tycho's SN1572	1572AD	7,500
Sagittarius A (E)	?	26,000
Veil Neula	>3600BC	1,400 – 2,600
Keler's SN1604	1604	20,000
Vela SNR	11th – 9th Millennium BC	800

Some of these sources are too difficult for the amateur to observe: either they are too weak or at too low a declination for observers in the UK. For example, Sagittarius A cannot be observed from the southern UK as it lies too close to the horizon, and ground noise will enter the antenna beam and mask the source. The easiest supernova remnants to detect are Cassiopeia A (Right Ascension: 23:23:21 & Declination: 58:49:59) and Taurus A – the Crab Nebula (Right Ascension: 05:34:30 & Declination: 22:00:57). Unfortunately they both lie close to the galactic plane and this can make it difficult to separate them out from the integrated galactic emissions. See Figures 8.1 and 8.2 [11].

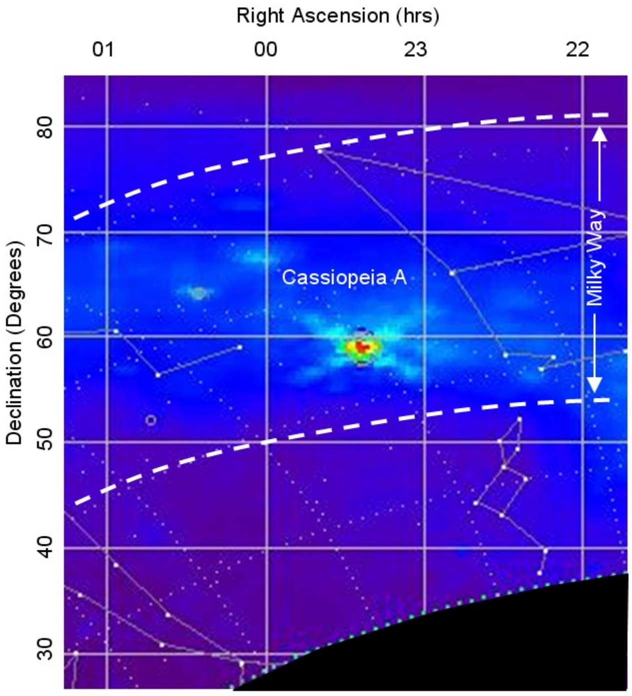

Figure 8.1 Location of Cassiopeia A

Cassiopeia A (3C461) lies in the outer edge of the galactic plane as seen from Earth. It is a very strong source at many wavelengths. In this picture from Radio Eyes [11] its intensity at 408MHz is given as 5500Jy.

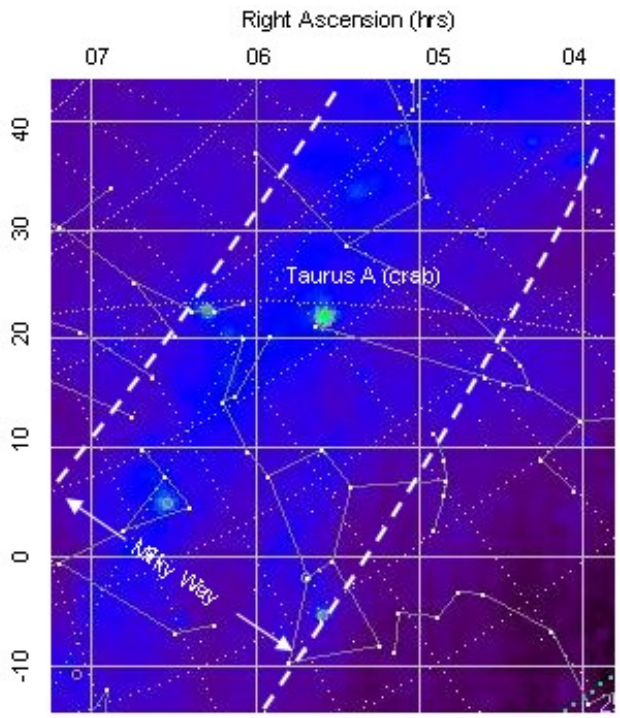

Figure 8.2 Location of Taurus A (Crab Nebula)

Taurus A (3C144) also lies in the outer galactic plane and has an intensity at 408MHz of around 1200Jy.

A good way to separate out point-like supernova remnant sources from the galactic background is to use a radio interferometer which will produce 'fringes' from the point source, but not from the widespread background. An example may be seen in Figure 8.3.

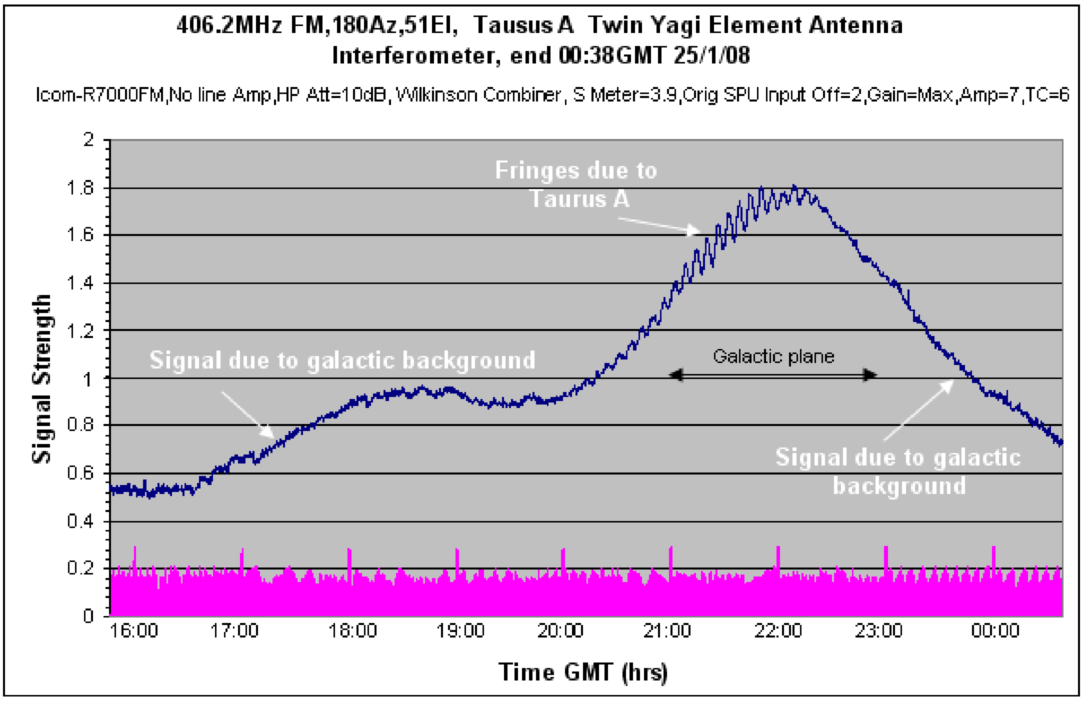

Figure 8.3 Separation of Taurus A from galactic background

Note that the 'hump' on which the fringes sit is due to the background emissions from the galactic plane. The fringes can easily be separated out with software as shown in Figure 8.4.

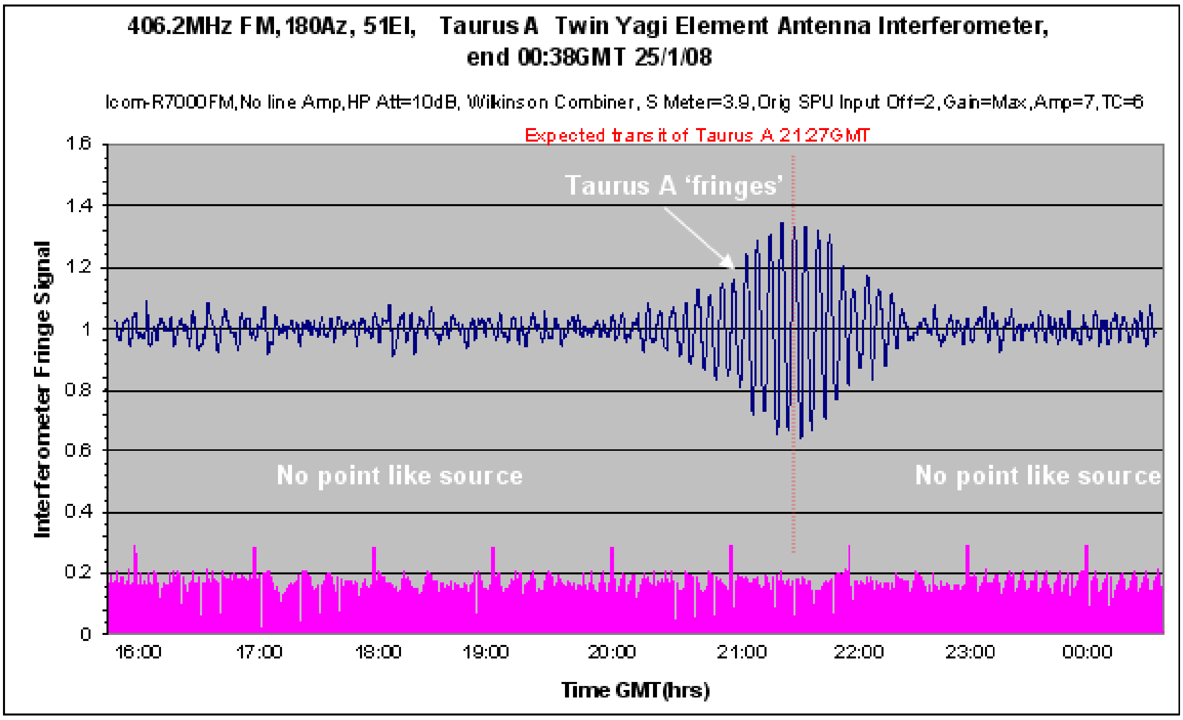

Figure 8.4 Amateur detection of the Crab Nebula

The Crab nebula supernova remnant is a beautiful visual and radio object. See Figures 8.5 & 8.6.

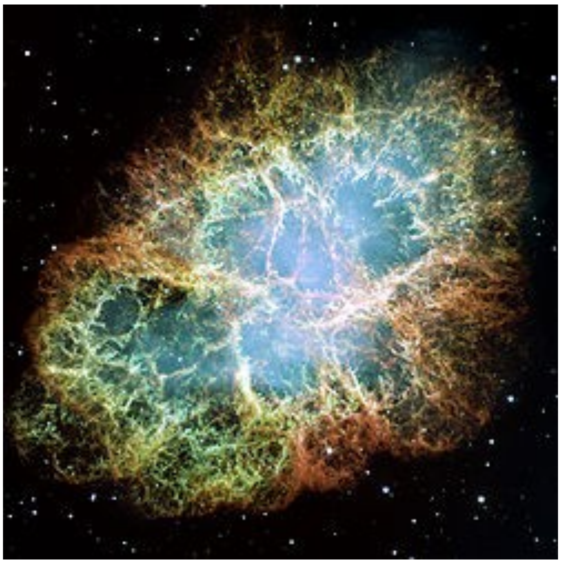

Figure 8.5 Crab Nebula (optical)

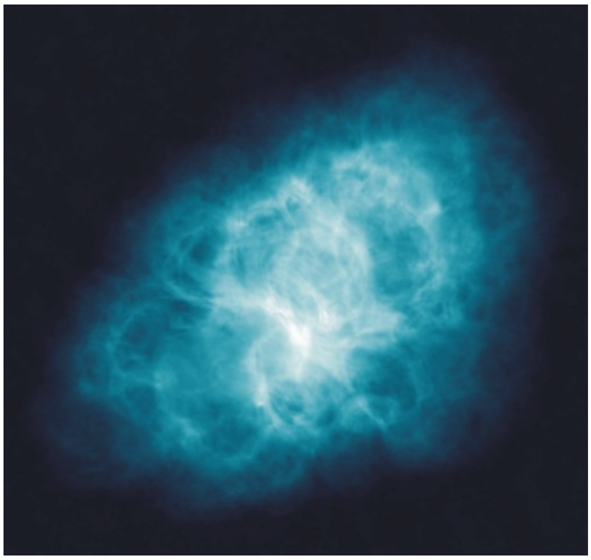

Figure 8.6 Crab Nebula Radio @ 5GHz

The remains of the original star has collapsed to a Neutron star and is a Pulsar spinning at 30 times at second and emitting its own special radiation pattern, but at levels much below that of the whole supernova remnant. Pulsars will be discussed in section 10.

References

1 J S Hey, The Radio Universe, Pergamon press

2 Palmer, Davies & Large, *Radio Astronomy Today*, Manchester University Press

3 http://www.radiosky.com/jupant1.html

4 http://www.moxonantennaproject.com/

5 radiojove.gsfc.nasa.gov/library/sci_briefs/decametric.htm

6 www.spaceacademy.net.au/spacelab/projects/jovrad/jovrad.htm

7 www.spacetoday.org/SolSys/Jupiter/JupiterRadio.html

8 http://www.radiosky.com/jupmodes.html

9 Stanford Chart software

10 http://scienceworld.wolfram.com/astronomy/GalacticCoordinates.html

11 Radio Eyes software *www.radiosky.com*

12 http://imagine.gsfc.nasa.gov/docs/science/know_l1/pulsars.html

13 http://www.naic.edu/~pulsar/gifs/wapp.gif

14 www.radioastronomy101.com/radio_astronomy_sections/attachments/1-13-Radio-Astronomy-Source-Verification.pdf

15 www.radio-astronomy.org/pdf/pulsars.pdf

16 www.radio-astronomy.org/

17 *www.radio-astronomy.org/pdf/pulsars.pdf*

18 Pulsar Radio Spectra - High Frequency Turnover
J. Kijak1,2, Y. Gupta2 and K. Krzeszowsk Chin. J. Astron. Astrophys., Vol. 6 (2006), Suppl. 2, 48–52 (*http://www.chjaa.org*)

19 *en.wikipedia.org/wiki/Cygnus_A*

20 *http://www.astronomycafe.net/anthol/w8s2.html*

21 D Morgan (unpublished) www.dmradas.co.uk

[The concluding Part 3 will appear in the next issue]

Cosmic Static*

RA Classics

GROTE REBER†, ASSOCIATE, I.R.E.

INTRODUCTION

IN 1932 Jansky[1] published the first of a series of papers[2,3,4] indicating that a certain type of static appears to come from space and in particular from the plane of the Milky Way. Very few other[5] data are available on the disturbance. Various[6] hypotheses have been advanced to account for the phenomenon but all have failed under quantitative calculation.

160-MEGACYCLE TESTS AT WHEATON, ILLINOIS

The writer became interested in this work about three years ago. It was decided to make measurements at various frequencies with equipment of high resolving power. The apparatus shown in Fig. 1 is really a transit telescope adapted to work at radio frequencies. The mirror is 31 feet in diameter and has a focal length of 20 feet. Details of operation have been given elsewhere.[7]

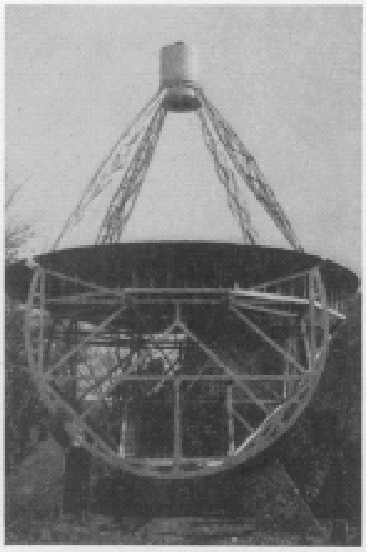

Fig. 1—Antenna system used for the investigation of cosmic static.

The output of the amplifier is indicated by the meter at the right of Fig. 2. When no radiation is present the reading is constant at some predetermined level. Any radiation captured will cause the meter to move in a downward direction. Readings are taken visually at minute intervals. A typical set of points is shown in Fig. 3. The dotted line across the dip in the curve is the condition that would have obtained had no radiation been intercepted. The input to the receiver is

$$\text{input} = \left[\left(\frac{\text{reference}+\text{deflection}}{\text{reference}}\right)^2 - 1\right] 8\times 10^{-18} \quad \text{watt/kc band} \qquad (1)$$

where "reference" is the number of microamperes corresponding to 8×10^{-18} watt per kilocycle band[4,8] and

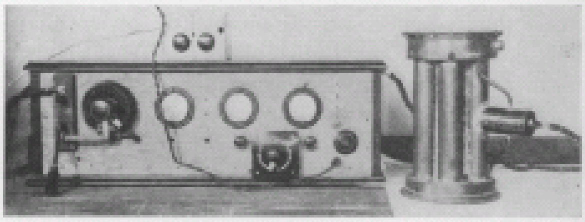

Fig. 2—Control and indicating equipment. The amplifier is shown at right.

"deflection" is the number of microamperes represented by the dip in the curve. The maximum recorded input is 15 per cent of the reference-level power and the band width of the receiver is about 10^3 kilocycles. The available input power, therefore, is 1.2×10^{-18} watt. The drum efficiency is 50 per cent, reflector efficiency

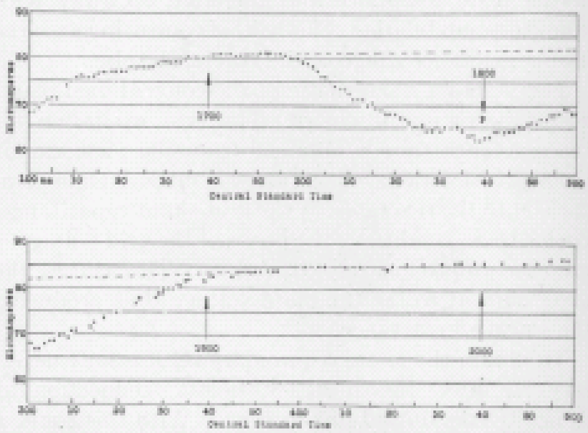

Fig. 3—Microamperes versus C.S.T. on May 11, 1939, for declination −20 degrees. Hours right ascension indicated by arrows. *P* marks the plane of the Milky Way. Galactic longitude for this declination is 337.2 degrees. The at first rapid, and later gradual, increase of reading is due to the warming up of the equipment.

* Decimal classification: R114. Original manuscript received by the Institute, September 8, 1939.

† Wheaton, Ill.

1 K. G. Jansky, "Directional studies of atmospherics at high frequencies," PROC. I.R.E., vol. 20, pp. 1920–1932; December, (1932).

2 K. G. Jansky, "Electrical disturbances of extraterrestrial origin, PROC. I.R.E., vol. 21, pp. 1387–1398; October, (1933).

3 K. G. Jansky, "A note on the source of interstellar interference," PROC. I.R.E., vol. 23, pp. 1158–1163; October, (1935).

4 K. G. Jansky, "Minimum noise levels obtained on short-wave radio receiving stations," PROC. I.R.E., vol. 25, pp. 1517–1530; December, (1937).

5 H. T. Friis and C. B. Feldman, "A multiple unit steerable antenna for short-wave reception," PROC. I.R.E., vol. 25, pp. 841–917; July, (1937); *Bell Sys. Tech. Jour.*, vol. 16, pp. 337–419; July, (1937).

6 Greenstein and Whipple, "The origin of interstellar radio disturbances," *Proc. Nat. Acad. Sci.*, vol. 23, pp. 177–181; March, (1937).

7 G. Reber, "Electric resonance chambers," *Communications*, vol. 18, pp. 5–8; December, (1938).

8 F. B. Llewellyn, "Limits to Amplification," *Bell Sys. Tech. Jour.*, vol. 14, pp. 85–95; January, (1935).

[Editor's note: Again, license enabled by anonymous sponsorship]

85 per cent, and area of mirror 7×10^6 square centimeters. This gives a maximum radiation intensity of 4×10^{-21} watt per square centimeter or equivalent to the energy arriving from a star of 22.1 balometric magnitude which indicates some of the technical difficulties encountered.

The acceptance cone of the mirror is about 3 degrees in diameter so the maximum absolute intensity of radiation becomes 4.5×10^{-25} watt per square centimeter per circular degree per kilocycle band. When intensity is plotted versus galactic longitude the points of Fig. 4 result. The rest of the directions around the Milky Way will be measured during the coming year as they arrive in good position.

The amplifier of Fig. 2 consists of five stages of acorn tubes tuned by concentric lines to the signal frequency. The last stage works into a diode detector which actuates a direct-current amplifier with a microammeter in the plate circuit. An increase in input will cause an increase in bias and a resultant decrease in the microammeter reading. In actual operation the amplifier is on the end of the drum in Fig. 1 and the direct bias voltage is fed down the cable to control the equipment.

Perhaps it is well to point out that cosmic static is in no way connected with cosmic rays. The latter are high-speed particles and have no directional effect except a 1 per cent increase on the leading face of the earth as it moves through space.

Radiation of Charged Particles

Considerable material is being thrown off by the stars. This expands and tends to fill up the region between the stars with a very tenuous gas. Since the gas is at a much lower density than the best artificial vacuum the particles are relatively far apart. Under the action of starlight these atoms of gas are ionized or free electrons are ejected with a velocity dependent upon the color of the light involved. Therefore space is filled with positive particles and high-speed electrons (of a few volts energy).

These particles may encounter in a variety of ways. The one of interest here is a free-free transition; that is an electron approaches a positive charge from one direction and is acted upon to leave in another direction. In 1923 Kramers[9] deduced from classical electric theory that when an electron encounters an ion in such a free-free transition energy will be radiated at the expense of the velocity of the electron. Eddington[10] applied Kramers' theory to the material inside a star. At that time he argued a certain correction due to Einstein should not be applied to Kramers' formula. This correction takes into account the stimulation of such radiation due to the transition occurring in equilibrium with an electromagnetic field. Later Eddington[11] applied Kramers' theory to the material of interstellar space with the specific argument that the average velocity loss of an electron due to free-free transitions could not exceed 12 per cent. In 1930 Gaunt[12] rederived Kramers' formula on the basis of quantum mechanics. He decided that Kramers' work is correct for visual range, too high for the X-ray range and too low for the low frequencies. Since no application was known he did not go into the low-frequency case in detail but definitely stated Kramers' formula does not include the effect of stimulated radiation. Partly on this authority and partly to fit the theory to measurements this correction is included in what follows.

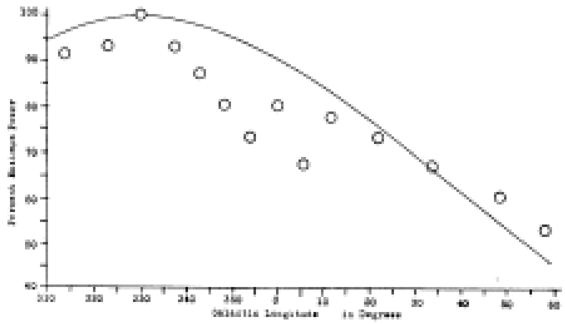

Fig. 4—Intensity versus Galactic longitude *l*. Circles indicate measured points. Solid line computed from equation (7).

Quantitative Calculations

Kramers gives the amount of energy liberated as

$$\rho = \frac{32\ \pi^2 Z^2 e^6}{3\sqrt{3}\, C^3 m^2 U}\, ns\Delta\nu \text{ ergs/cm}^3\text{/sec} \qquad (2)$$

where

- n and s are numbers of electrons and ions per cubic centimeter
- e, m, and U are the charge, mass, and velocity of the electrons
- Z is the atomic number
- C is the velocity of light
- $\Delta\nu$ is the band width

The correction[10] for stimulated radiation may be reduced to incremental form such that true radiation becomes

$$\rho' = \frac{kT}{h\nu}\, \rho \text{ ergs/cm}^3\text{/sec} \qquad (3)$$

where

- k is Boltzmann's constant
- h is the Planck's constant
- T is the effective temperature of the electromagnetic field (3.2 degrees absolute for space)
- ν is the frequency in question

[9] H. A. Kramers, "Theory of the continuous X-ray spectrum," *Phil Mag.*, vol. 46, pp. 836; November, (1923).

[10] A. S. Eddington, "Absorption of radiation inside a star," Monthly Notices of Royal Astronomical Society, vol. 84, p. 104, (1924).

[11] A. S. Eddington, "Diffuse matter in interstellar space," *Proc. Royal Soc.*, vol. 111, pp. 424, (1926).

[12] Gaunt, "Continuous absorption," *Trans. Royal Soc.*, vol. 229, pp. 163, (1930).

Eddington[11] evaluated ρ as $\rho = 8.7 \times 10^{-42}\, \Delta\nu$ erg per cubic centimeter per second; therefore ρ' becomes

$$\rho' = 5\,84 \times 10^{-31} \frac{\Delta\nu}{\nu} \text{ ergs/cm}^3\text{/sec.} \qquad (4)$$

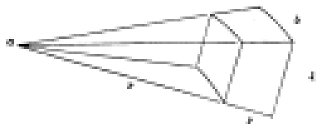

Fig. 5—Incremental volume used in calculation of radiation intensity.

Consider now the situation shown in Fig. 5. The incremental volume will be (when the angles are small)

$$\Delta V = r\Delta b\, r\Delta l \Delta r = r^2 \Delta b \Delta l \Delta r. \qquad (5)$$

The incremental energy arriving at 0 from this incremental volume is

$$\Delta I = \frac{\rho'}{4\pi r^2} \Delta V = \frac{\rho'}{4\pi} \Delta b \Delta l \Delta r. \qquad (6)$$

Integrating from zero to r centimeters gives an absolute intensity at 160 megacycles of $7 \times 10^{-41} r$ erg per second per square centimeter per circular degree per kilocycle band.

Astronomical Interpretation

Consider the geometry of Fig. 6 where

$$r = d \cos l + (d^2(\cos^2 l - 1) + c^2)^{1/2} \qquad (7)$$

c = radius of the Milky Way
d = distance from the sun to the center
l = galactic longitude
r = distance from the earth to the edge of the galaxy.

The way r varies with l depends upon the ratio of d to c. The relation giving best fit to points is when $d = 2c/3$ and is shown by a solid line in Fig. 4. Dividing the observed maximum absolute intensity by the absolute intensity due to radiation from charged particles gives a maximum r of 6.5×10^{22} centimeters or 2.1×10^4 parsecs. The radius of the galaxy then becomes 12,600 parsecs.

Other Data

Various bright stars such as Vega, Antares, etc., have been tried but no measurable response was obtained. Repeated attempts to measure radiation from Mars were also of no avail. While some fine structure of radiation pattern seems to be present the existing equipment is not adequate for its accurate resolution. No conclusive measurements have been made on any of the extragalactic nebulae; however, these are to be worked on next. Tests on the sun are always under rather unfavorable conditions but if radiation occurs from this body it is of intensity below 4×10^{-24} watt-per-square-centimeter-per-kilocycle band at 160 megacycles.

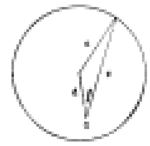

Fig. 6—Plan view of the Milky Way. Earth and sun at point O.

In the beginning it was hoped (from the theory of black-body radiation) that the intensity would increase as the square of frequency. Therefore the first tests were made at 3300 megacycles with rather crude equipment. Nothing was found at the sensitivity limit of 10^{-20} watt per square centimeter per circular degree per kilocycle band. Better apparatus for a frequency of 900 megacycles also produced no positive results at a limit of 10^{-22} watt per square centimeter per circular degree per kilocycle band. These negative results point to a function for ρ' similar to the above.

The only other data amenable to calculation is that of Jansky's original paper. Taking into consideration the ground reflection[13] and assuming the Milky Way to have a thickness through the center of one tenth the diameter his maximum measured intensity will produce a radius of 13,100 parsecs and an eccentricity of 3/4 radius for the earth which is a good check on the inverse-frequency function of ρ'. It is also worthy of note that Plaskett in a recent paper[14] deduces a most probable radius of 15,000 parsecs for the Milky Way so these figures are in fair agreement.

[13] C. B. Feldman, "The optical behavior of the ground for short radio waves," Proc. I.R.E., vol. 21, pp. 764–801; June, (1933).
[14] J. S. Plaskett, "Modern conception of the stellar system" *Pop. Astronomy*, p. 293, May, (1939).

[*Editor's notes:*

Yes, this is the seminal paper that started it all, the second after Jansky's paper of 1932 ! Note that this was in the Proc. IRE, the forerunner of the Proc. IEEE i.e. it was published by a radio/electrical/electronics journal, not by one on astronomy. That came the same year, essentially the same as the above. Remember that Reber's typical day of observation included 9 hours at work in the Chicago radio plant, a 45 min. commute, supper, sleep from 7 p.m. to midnight and observations (without paper recorder initially) until dawn. For more details of this remarkable pioneer, my hero, see the account in Sullivan's superb book Cosmic Noise (see issue 1 of RAGazine.]

Low Cost Hydrogen Line Radio Telescope using the RTL SDR - Phase 2

Peter W East

H line, low cost technology

Abstract

Detecting the hydrogen line in the arms of our galaxy using modern technology is now easy. Key available components are low-noise RF amplifiers and software-defined radio (SDR). With a home-made Yagi, a couple of amplifiers, a cheap RTL2832U TV dongle, a bit of effort and some free software, for well less than £200 you can be up and running measuring the velocity and positions of the spiral arms, some tens of thousands of light years away. This paper describes the phase 2 upgrade, improving both the receiver and the antenna, now mountable on a tracking telescope mount, able to position the antenna for serious galactic equator measurement. Early results show good repeatable performance, and with a bit of mathematics plots some arms of our galaxy.

Introduction

In the basic receiver paper[1], it was recognised that improved antenna directivity was worth striving for. In addition in the upgrade, more RF gain was added to better utilise the SDR ADC range and extra RF filtering added to minimise interference. The new antenna construction design was aimed to make it compatible with a driven equatorial telescope mount (Celestron CG-5 Advanced GOTO Computerized Mount, ~£500). A home-made Alt/Az timber structure was considered, but the lure of GOTO to automatically direct the antenna accurately and painlessly was deemed worth the cost.

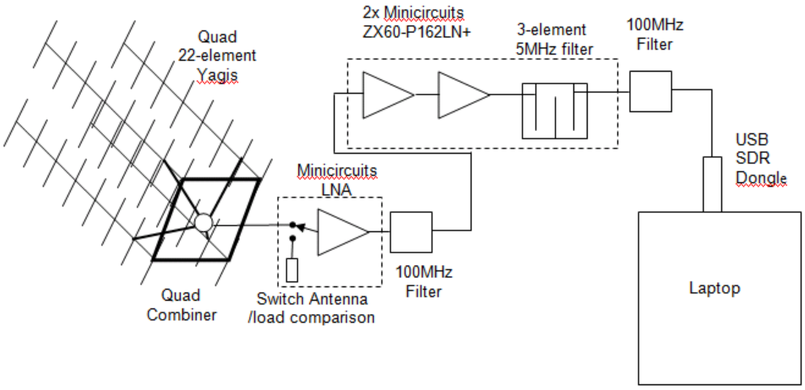

Figure 1. Simple Radio Telescope Upgrade

Figure 1 shows the upgrade schematic. The receiver is boxed in two units, one closely attached to the antenna and the second, remotely near the SDR/Laptop processor.

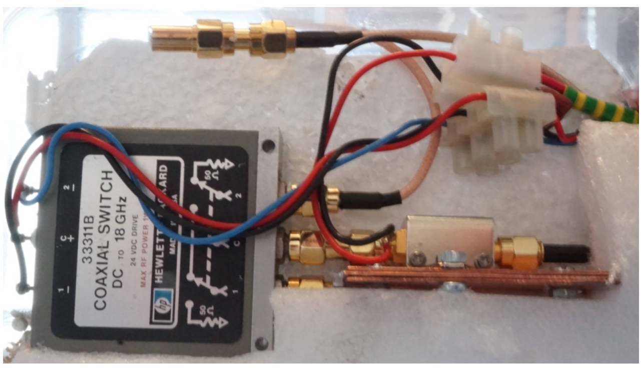

Figure 2 Switch/Preamplifier Unit

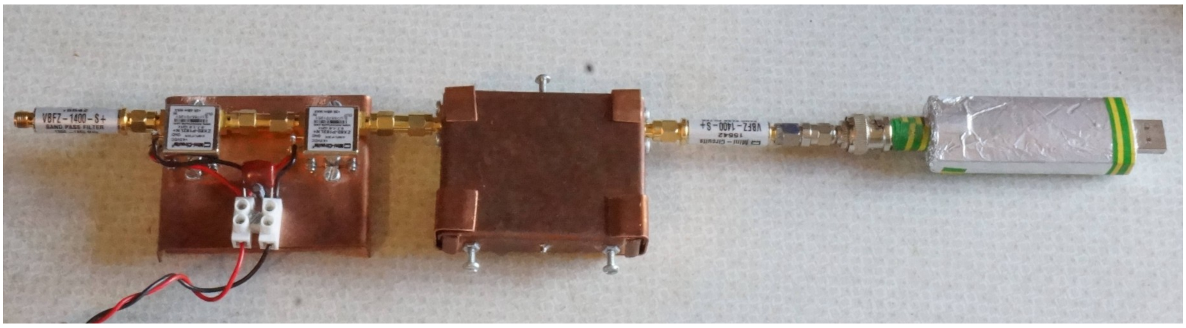

Figure 3 RF Filter/Amplifier/SDR Unit

The RF units shown in Figures 2 and 3 are normally boxed and shielded. Most of the components such as the switch, load and the 5MHz narrow-band filter are as used in the previous article [(1)]. Figure 3 also shows the 100Mhz filters supplied by Miniciruits (£30 each), which were shown to be necessary to cope with neighbouring high power PC's. These could also have been produced using the 5MHz filter design package[(2)].

Antenna (£50)

The antenna upgrade (Figure 2) involved a redesigned Yagi in a quad array, but still based on the original design. Again it was designed using P. McMahon's YagiCAD[(3)] starting with the DL6WU20 file in the software 'Example Models' list. For this design, the software was used to optimise the design at 1420MHz by tuning the centre frequency lower to 1390MHz and using the wide band optimiser and displays to improve the gain, match and back-lobes at 1420MHz. Beamwidth now is around 13deg and gain about 24dB. Figure 4 shows the antenna with an inset detail of the construction. The booms comprise bolted back-to-back 9.5mm aluminium U-channel 1.5m sections. Bronze welding rod 1.6mm diameter elements are clamped between the U-sections, predrilled and insulated with heat-shrink sleeving. The driven dipoles are similarly clamped but mounted in drilled perspex rod.

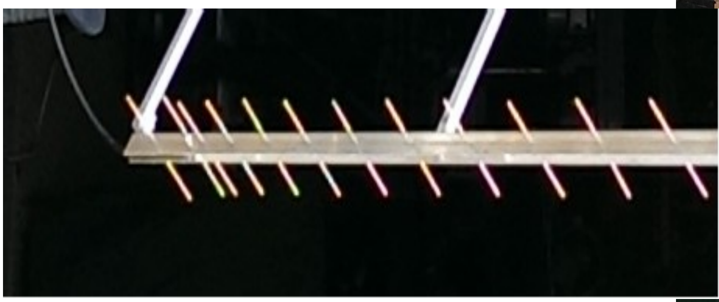

Figure 4. Quad Yagi Array on C-5 Mount

The array is balanced and supported by 1" square tube which slots over a 3/4" bar and plate mounting structure.

Antenna Combiner - 3 versions

1. Coaxial line 1/4 wave transformers - home-cut coax lines

In Figure 5a, paralleling the upper two antennas drops the impedance to 25Ω, the 50Ω quarter-wave transformer converts this to 100Ω. Similarly for the lower pair of antennas. Combining the two quarter-wave lines halves their 100Ω output impedances to 50Ω, matching the output 50Ω transmission line.

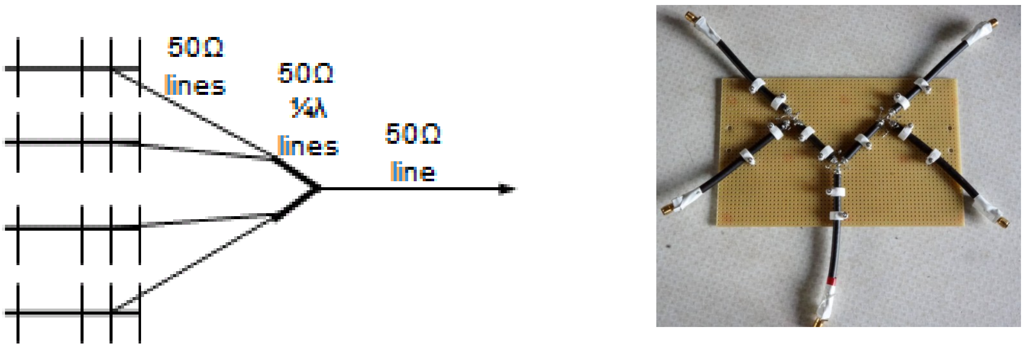

(a) (b)

Figure 5. Combining Four 50Ω antennas.

2. Coaxial line 1/4 wave transformers - connector assembly

An alternative to cutting and soldering lengths of coax, is to assemble SMA connectors and adapters to good approximation as shown in Figure 6. Various adapters are used to adjust the arm lengths to 1/4 wavelength.

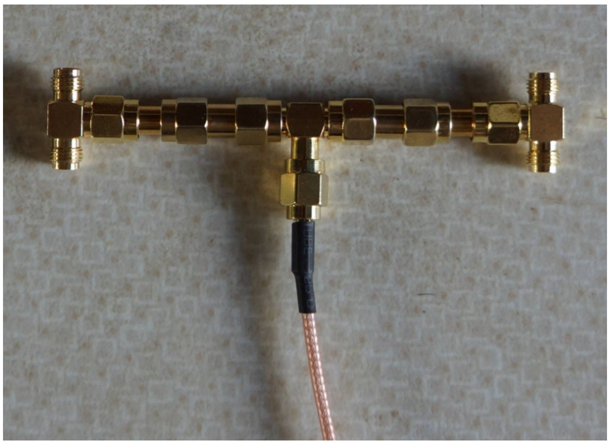

Figure 6. Connector combiner

3. Power Divider/Combiners

Matched combining using commercial power combiners, is best tolerant of Yagi source mismatches as shown in Figure 7.

Figure 7. Power Divider/Combiner

Minicircuits sell a combiner for this band (~£50) but some are available from China on ebay for £15. Comparing these three options in place, case 3 gave the most consistent results but insertion loss and system temperature was highest, case 2 gave the least loss, but in both cases 1 and 2 mismatch differences between the Yagis was evident but some tuning of a Yagi driver element length improved the situation. It is concluded that with the right test equipment, in both cases 1 and 2 1/4-wave transformers could be optimised to cope with antenna manufacturing and design differences and give the lowest system temperature

SDR Receiver (£10)

The Realtek RTL2832U DVB-TV dongle (RTL) is compatible with SDR# software[4] and needs the Zadig[5] driver for WINDOWS. For Hydrogen line astronomy, the SDR# spectrum displays are not very useful containing only time-constant variable attack and decay on FFT bins. However it is very useful for locating interfering sources and checking efficient and proper operation of the receiver/RTL SDR.

Once the system has been checked, data is collected using the OsmoCom 'rtlsdr' library & capture tools[6]; the data files contain raw IQ data for later analysis. Versions are available for both Windows and Linux. Data analysis uses the *RAFFT.exe*[7] FFT averager program for Windows or *rafft*[8] for Linux.

Two versions of the RTL2832U dongles have been compared, one using the E4000 tuner and the other - more commonly available now at very low cost - using the Rafael 820T tuner.

SDR Operation

Radio astronomy applications for SDR's require operation in a different regime to normal broadcast radio. For example, in conventional receivers, AGC is a common method to ensure that demodulation occurs in the optimum signal range and copes with variations of reception conditions and siting relative to transmitters. Radio telescopes on the other hand require constant gain, adjusted to an optimum for the target of interest, although there are cases where AGC is applied to the reference channel for Dicke switch reception.

With digital SDR's and conventional use, it is normally sufficient for RF/IF gain to be set so that system noise levels just exceed the minimum ADC threshold so that for most signals, the majority of the ADC amplitude range is available for the wanted signal. In radio astronomy, to minimise the effects of quantisation noise, the whole ADC dynamic range should encompass the noise-like target/reference amplitude response range. This means that the RF amplifier chain and SDR IF gains need to be adjusted to ensure this applies. For H-line measurements this overall gain is typically around 90 to 100dB.

The software program *ASTATS.EXE*[9] for Windows (*astats*[10] for Linux) gives a graphical view of the ADC operating amplitude distribution. The instructions in DOS / Linux terminals are of the form:

Windows: ASTATS.EXE <infile.bin> <outfile.txt>
Linux: ./astats <infile.bin> <outfile.txt>

The output text file showing the ADC amplitude distribution can then be displayed in Excel type spreadsheets or MathCad packages. The x-axis represents the ADC byte value and the y-axis the normalised byte value count. Figure 8 shows some typical reference load *.bin* records.

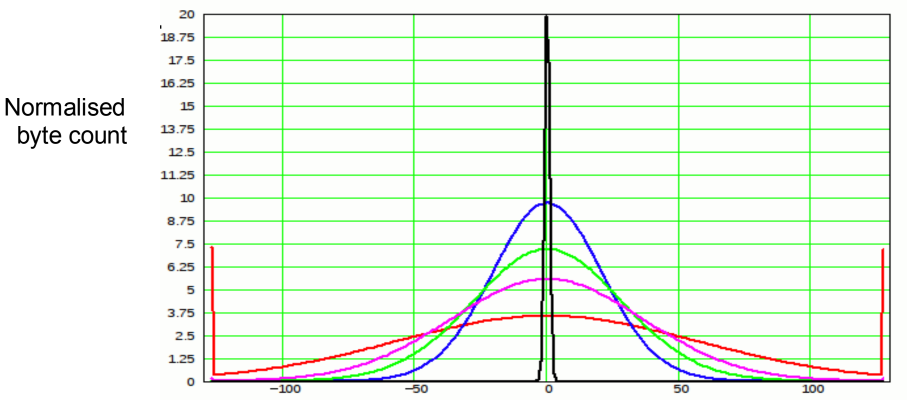

Figure 8 Some typical ADC amplitude distributions

Examples blue and green in Figure 8 are acceptable; magenta and red show evidence of limiting at the ADC positive and negative extremes, possibly producing spikes in the resulting FFT. Insufficient RF gain is indicated by narrower spikes (black) around value zero point.

Measurements

Measurements summarised in Figures 9 and 10 were made at 0° Galactic latitude and at 10° longitude intervals over the visible galactic plane from 80° to 180°. Right Ascension and Declination values for directing the equatorial mount to chosen Galactic Latitude and Longitudes were obtained from an online Universal Coordinates Converter[11].

Each data set comprised 200 x 10^6 samples taken over about 100 seconds. Data sets (see Appendix) were split into 256 sample blocks, the signal spectrum extracted using 'rafft' program and all FFT block sets averaged. Similarly for reference load measurements.

Output longitude spectra were then divided by the average of seven 100sec reference load spectra, so providing the ratiometric[1,12] hydrogen line ratio responses shown in the figures.

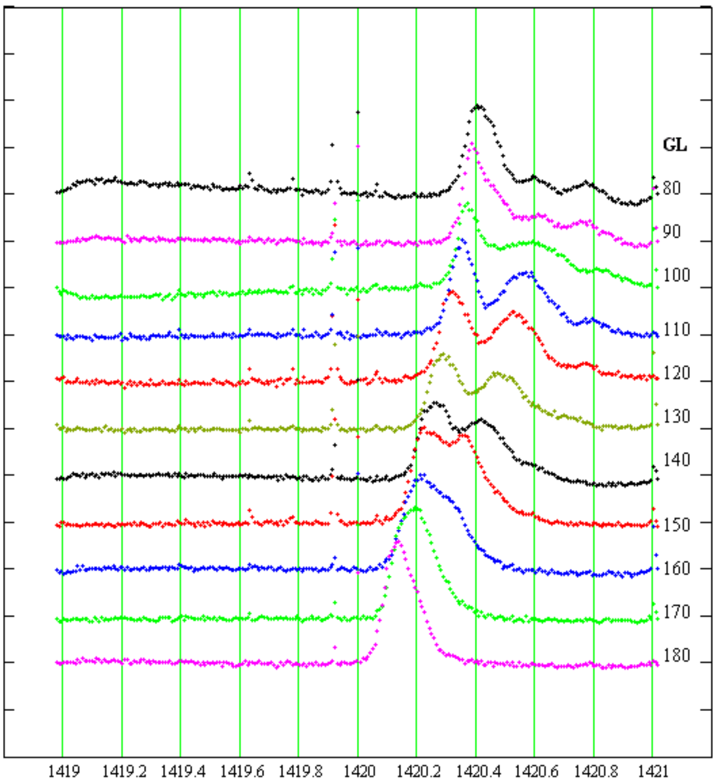

Figure 9. Spectral Display Measurements
Galactic Latitude 0°,
Galactic Longitude as marked

These raw results are as recorded; the frequency migration of the largest peaks (local arm) with angle is real and due the Earth/Sun platform vector velocity of the Local Standard of Rest (VLSR).
Correction velocities vary with the RA and Dec, and also with time. So each data set needs specific corrections, available from online calculators; Reference (13) was used for this project.

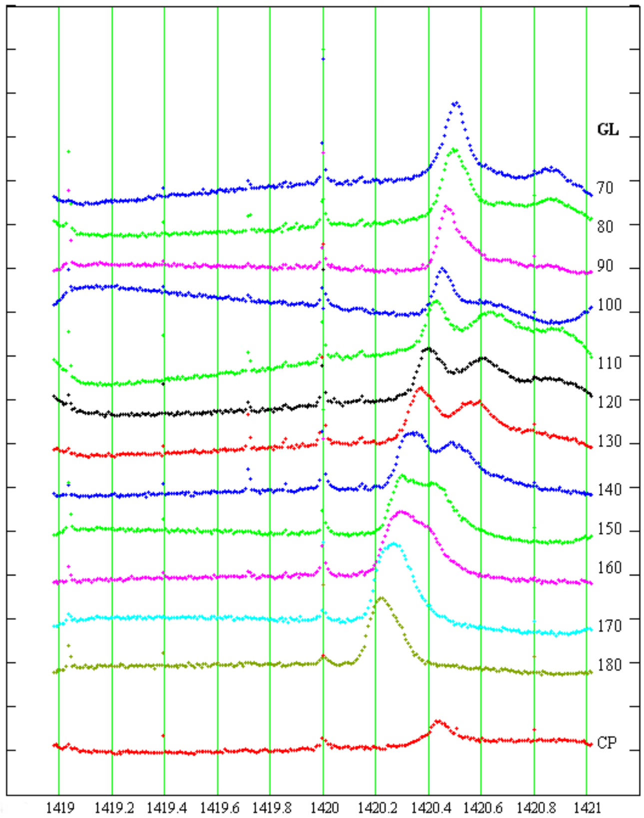

Figure 10. Spectral Display Measurements Galactic Latitude 0°, Galactic Longitude as marked

Included at the bottom of Figure 10 ('CP') is a plot with the antenna pointed to the Celestial Pole, where it might be expected that Hydrogen line Doppler shift may be low and therefore provide a reference calibration.

Comparing Figures 9 and 10, it is clear that galactic longitude spectral measurements correlate well, although there is obviously an SDR-associated frequency offset. Both SDR's needed calibration correction, E4000 of 25kHz and the 820T of 100kHz. Some external interference is evident affecting baselines of Figure 10 at GL < 130°

Plotting Galaxy Arms

Assuming the spectral peaks represent the centres of hydrogen clouds in the galaxy spiral arms, their positions can be calculated from the geometry of Figure 11. Given knowledge of the galaxy rotation rate (assumed constant with radius) and spectrum peak frequency/doppler velocities versus longitude, this is sufficient information to solve the triangles in Figure 11 to estimate the ranges to the corresponding spiral arms' hydrogen clouds.

A calculation example for GL = 120° is given to illustrate the method. Firstly the spectral peak frequencies need to be converted into Doppler velocities:

$$v_{doppler} = c.f_{doppler}/f_s = c.(1420.406 - f_{peak})/1420.406 \sim 211\text{km/s/MHz}$$

(c is velocity of electromagnetic waves = 3×10^8 m/s)

At Galactic Longitude 120°, the three frequency-corrected velocities at the three spectrum peaks of Figure 9 are -96.8km/s, -44.5km/s, and 0km/s.

If V_{rot} is the mean rotation rate of the galaxy over the region containing the sun and galaxy arms of interest. V_{rot} ~220km/s, we can calculate the sun velocity in the direction of the hydrogen clouds from,

$V_s = V_{rot}\cos(120\text{-}90) = 190.5$km/s.

The three cloud velocities are then:

Local arm: $V_0 - V_s = -0$km/s, therefore $V_0 = 190.5$km/s
Perseus arm: $V_1 - V_s = -44.5$km/s, therefore $V_1 = 146$km/s
Outer arm: $V_2 - V_s = -96.8$km/s, therefore, $V = 93.7$km/s

For the Perseus arm, using, $R_1/\sin(120) = R_s/(V_1/V_{rot})$, then, $R_1/R_s = 1.507$
(this equation substitutes the relation, $V_1/V_{rot} = \cos b_1$, where b_1 is the angle between the vectors V_{rot} and V_1 in Figure 11).

For the Outer arm, using, $R_2/\sin(120) = R_s/(V_2/V_{rot})$, then, $R_2/R_s = 2.348$
The position of the clouds lie on the coordinates $R_1\cos[b_1 - (120\text{-}90)]$, $R_1\sin[b_1 - (120\text{-}90)]$ by substituting the sun-galactic centre (~ 30kly) range; similarly for the local and outer arms.

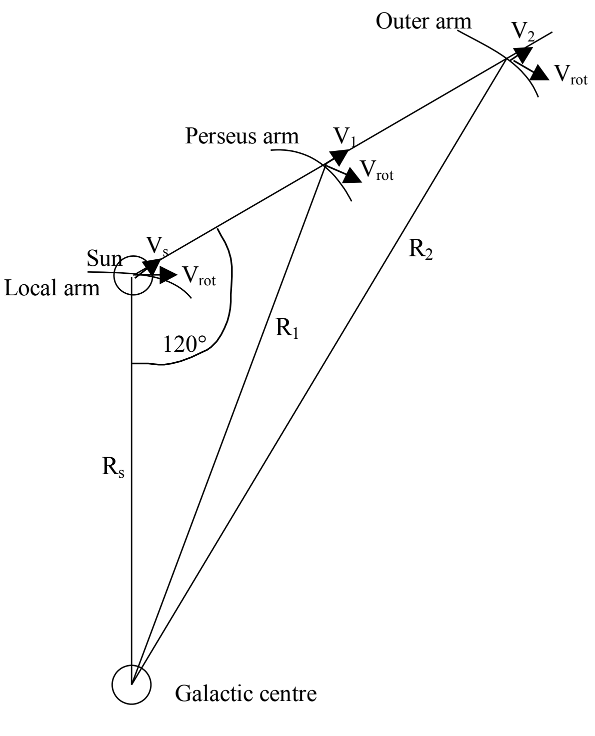

Figure 11. Plotting Galaxy Arms - example longitude 120°

Figures 12 and 13 summarise galaxy arm plots using data from Figures 9 and 10, after frequency calibration and corrected for the Earth's relative velocity in space using an online calculator(12) to derive the velocity of the Local Standard of Rest (VLSR).

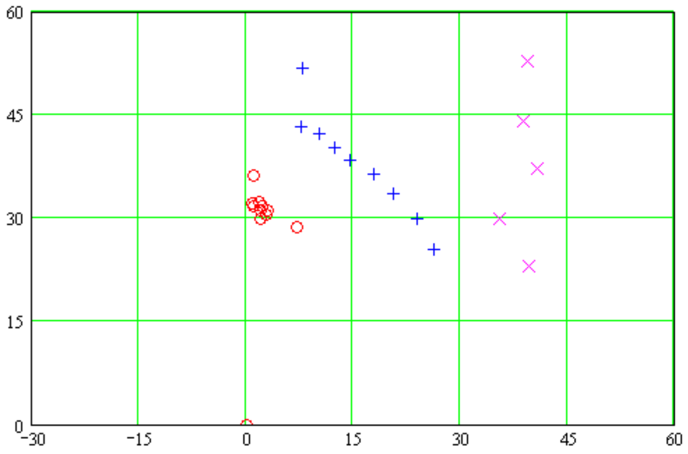

Figure 12. Galaxy arms plot using the SDR 820T tuner

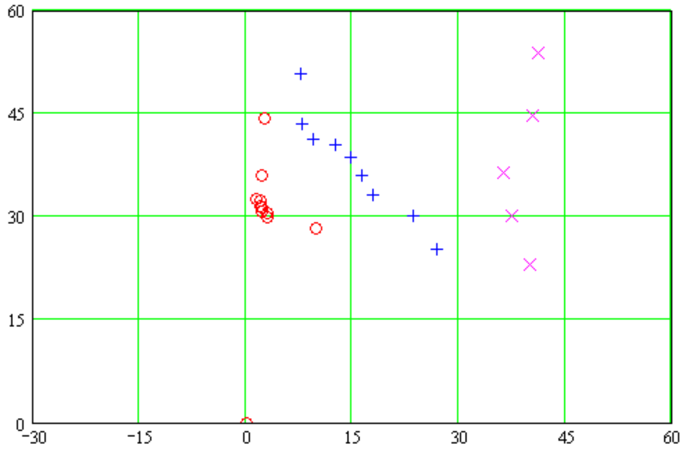

Figure 13. Galaxy arms plot using the SDR E4000 tuner

Figures 12 and 13 offer views of the presence of the spiral arms of our galaxy over a 90° galactic longitude sector based on manual identification of spectrum peaks in the analysed data presented in Figures 9 and 10. Although crude, trends are illustrated, although the calculations suffer from various inaccuracies. These include noise in the spectra amplitudes affecting peaks, the broad spectral lines due to dispersion in the clouds, and the wide longitude smoothing from the relatively broad antenna beamwidth. In addition, the geometrical calculations around 180° are not so tolerant of data and rotation rate errors.

Conclusions

It is interesting that with such a basic receiver and small antenna it is possible to observe hydrogen clouds in our galaxy arms some 45,000 light years away. A comparison of these charts with professional versions shows that they are crudely comparable.

The main difficulty in achieving these results is coping with local interference. Without the added 100MHz filters, at times the receiver was swamped and no hydrogen data was visible. In getting these results, it was apparent that receiver gain drift affected the baseline level. Drift was evident between successive measurements, so some form of temperature control or receiver architecture changes would be necessary to achieve more stable results. The SDR# software[4] was useful in locating local interference.

More information available at http://www.y1pwe.co.uk/RAProgs/index.html

References

1 http://www.britastro.org/radio/projects/Low_Cost_H_Line_Telescope.pdf
2 http://www.wa4dsy.net/cgi-bin/idbpf
3 http://www.yagicad.com/YagiCAD/YagiCAD.htm
4 http://www.sdrsharp.com/index.php/downloads
5 http://zadig.akeo.ie/
6 http://sdr.osmocom.org/trac/wiki/rtl-sdr#

7 http://www.y1pwe.co.uk/RAProgs/RAFFT.exe

8 http://www.y1pwe.co.uk/RAProgs/rafft
9 http://www.y1pwe.co.uk/RAProgs/ASTATS.EXE
10 http://www.y1pwe.co.uk/RAProgs/astats
11 http://hea.iki.rssi.ru/AZT22/ENG/cgi-bin/c_prec4.htm
12 http://www.y1pwe.co.uk/RAProgs/Ratiometric Dicke Radiometer.doc
13 http://www.jupiterspacestation.org/software/Vlsr.html

Appendix - Post Processing for Linux

Information on setting up the OsmoCom rtl tools is given in Reference (6). Copy 'rafft' to your working Data directory. The programs are run in Linux terminals. The procedure for this is described below.

1 Set up your Data directory on the Desktop.

2 Open a terminal and change directory to the Data directory

3 To record data to .bin files, type on the command line…
rtl_sdr ./capture1.bin –f 1420e6 –s 2048e3 –g 42 –n 200e6 -tunes
which sets the frequency to 1420MHz,
samples both I and Q ADC's at 2.048MHz, sets dongle gain at 42dB and records 200 million I and 200 million Q samples interlaced in the output file.
The output file capture1.bin is stored in the 'Data' folder

4 Open a second terminal and change directory to the Data directory

5 To perform and average 256-point FFT spectra, type on the new terminal command line …. *rafft capture1.bin capture1.txt 256*
The output capture1.txt file stored in the current directory can be input to Excel/ Spreadsheet or any math cad program to compare pairs of load and antenna files to view the hydrogen line spectrum.

Build your Own Yagi Antenna

Bob Kerswill (M0KER) & Paul Hyde (G4CSD)

Antenna, DIY meteor scatter

This article is a guide to how an absolute beginner can build a low-cost antenna suitable for the GRAVES frequency (143.05 MHz) and to give some simple tips and guidance and provide inspiration to have a go at building your own equipment. The intention is to illustrate a variety of different construction techniques rather than specific designs.

Based upon the ‘G4CQM MetScat’ design by Derek Hilleard, several versions have been built independently by the joint authors and tested and found to work without any setting up, thus dispensing with the need to use test equipment. It’s an attractive design because it is simple, relatively compact and has a broad response, making it tolerant of minor variations in manufacture. Further information on the predicted performance of the antenna can be found under the ‘Featured Builds’ section of Derek Hilleard’s website at http://g4cqm.www.idnet.com/HOME/index.html

All the materials used were purchased from well-known DIY retail outlets for under £15 excluding the connecting cable. Simple basic tools are all that are required. The construction techniques are open to interpretation as long as the lengths and spacing of the elements are observed. As with any DIY project you should have the skills and awareness of basic safety measures to proceed.

The G4CQM MetScat Design

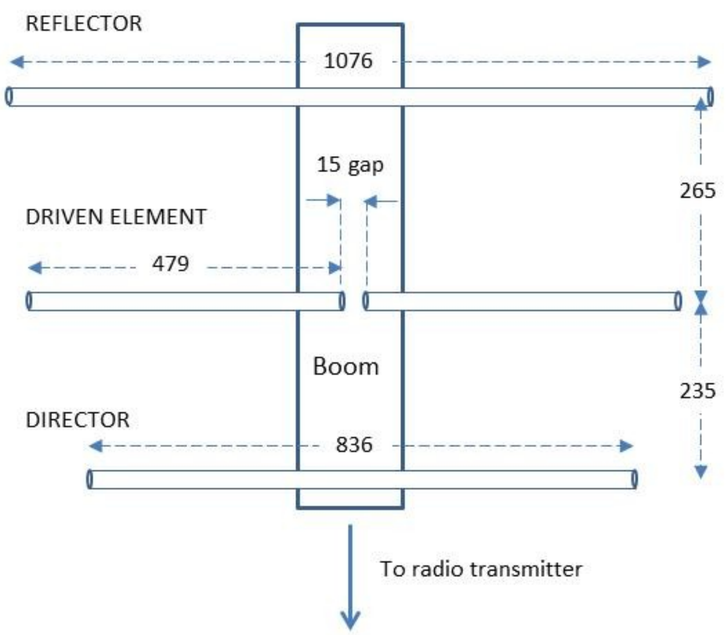

The basic design is known as a Yagi - Uda (or just Yagi) antenna with a central ‘boom’ and three ‘elements’.

The boom is only there to support the elements, and the dimensions are not critical, although it must be sturdy enough to withstand high winds and must provide a means of attaching the antenna to its support.

The dimensions have been calculated for elements made of 15mm or 5/8 inch OD copper or aluminium pipe.

All dimensions shown are in mm.

Construction Techniques

We will consider the options open in terms of the main components of the antenna. You can chop and change between the different techniques depending upon what you have in your scrap box or can easily obtain from local stores. Remember, the only critical thing is that the elements are the correct length and are spaced the correct distance apart.

Tips:

Remember that timber sizes are usually nominal, so check the actual dimensions when cutting etc. Do not assume that what is on the label is exact, and also look down the length before buying to ensure you get a straight piece.

Give the timber boom a couple of good coats of external grade varnish before mounting the elements etc.

Copper pipe is ideally cut with a pipe cutter to get a clean square cut, but a junior hacksaw serves just as well. But ensure the cut is square and that the ends are filed to remove any sharp edges. A simple way to get a clean square cut is to mark where the cut line is and then wind a piece of electrical insulation tape around the pipe and cut just above the tape edge and file down to it.

The Boom:

This needs to be a minimum of 550mm long and made preferably from a non-conducting material. Aluminium square section could be used but this will then entail extra work in insulating the antenna elements, so we will concentrate on using square or rectangular timber section which makes life a little easier, or the use of plastic conduit as a boom. So the next three images give some idea of the basic construction.

Antenna A uses a simple, well-varnished wooden batten for the boom. A longer boom allows the antenna to be fixed behind the Reflector, which is preferable if the antenna is to be fixed to a metal support.

Photo 1 left, photo 2 below

Antenna B has the Director and Reflector elements secured to the wooden boom by 15 mm holes drilled through the boom section, leaving a 1mm bridge. An additional cross-piece is then used to support the two halves of the Driven element.

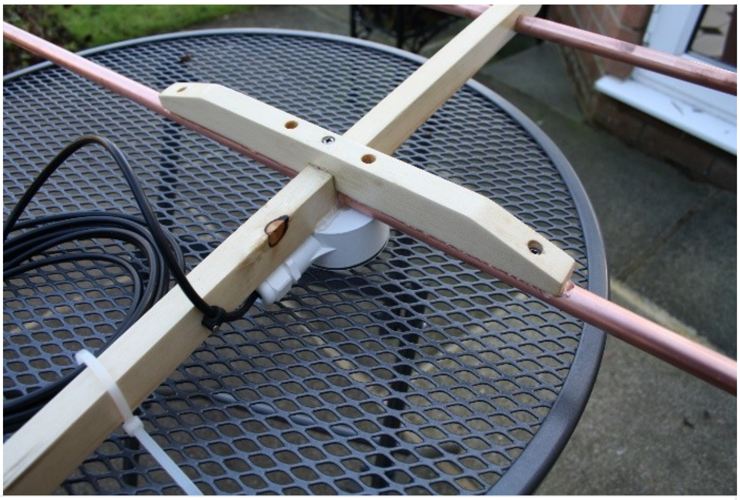

In choosing the timber to be used for the boom, one should consider not only the weight but also distortion. The section used for example in Antenna B is 28 mm x 18 mm. Think of how you are going to attach the antenna to the mounting bracket. The fixings will have to remain secure in high winds.

It's best to sand all edges and corners before applying the varnish. And when drilling to prevent breakout and splintering use a sharp drill of the appropriate size and do not apply excessive pressure to the drill. Let it cut its own way through the wood.

Antenna C uses cheap 20 mm diameter electrical conduit and junction boxes to form the boom and element supports, plus weatherproofing for the coax connection. These fittings are available in black plastic which reduces visibility compared to the white version. You may need to go to an electrical wholesaler for the four-way boxes.

Photo 3

The conduit forms a tight fit into the junction boxes but should still be glued in using pipe solvent adhesive. This does mean getting the dimensions absolutely right as you cannot adjust the spacing between the elements once glued. Use a dry run to check everything fits before you glue the central boom sections. When fitting the boom sections together do not use any twisting motion – you will never get the junction boxes to lie flat, so the antenna elements will not lie in the same plane. Instead place the boxes on a rigid, flat surface and push them together. A slight misalignment might be rescued by screwing the boxes onto a wooden boom, rather than throwing the whole thing away, but that does risk failure of one or more of the conduit connections. Covers and weatherproofing gaskets are available and should be fitted upon completion.

The Driven Element (or Dipole)

This is the area that needs the most thought because the two halves of the dipole need to be mechanically secure so that a roosting pigeon is not going to dislodge them, and because the electrical connections to the coaxial cable need to be weather proof and resistant to corrosion.

Antenna A and C driven elements are secured as shown in Photos 1 and 4.

In Antenna B the copper pipe is once again secured to the timber cross section by self- tapping screws from the underside, ensuring that both sections of pipe are correctly aligned. Silicon sealant is then applied to the pipe/timber intersection to improve weathering properties.

One important point in all examples is the need to seal the ends of the driven elements to prevent water entering the terminal box. This can be achieved either by sealing the open ends with silicon sealant, leaving it proud until set and then trimming square with a utility knife, or by purchasing a couple of 15 mm push on end caps. If you choose to use the copper solder type end caps remember this will increase the length of the elements slightly and change the characteristics of the antenna. So best to fix and solder the end caps first and then measure the exact length including the end cap.

Unlike the parasitic elements, the two driven elements are connected to a suitable receiver by means of a coaxial cable which is dealt with later. In order to effect a secure waterproof connection a weatherproof enclosure is required and the most suitable and readily available are the junction boxes used in 20mm plastic conduit systems. They are available in various configurations and a lid and gasket effectively seal the interior.

In both examples, a 20mm cable gland is inserted into the box and either glued in with the appropriate solvent or sealed in with silicon sealant. In both cases ensure that undue pressure is not put on this joint when tightening the gland nut. Try to get a gland that is suitable for 5-7 mm overall diameter cable. If you can only get hold of the standard glands it will be necessary using electrical insulation tape to increase the diameter of the coaxial cable at the point of entry into the gland. If using Antenna C then the same approach is used but the cable gland and cable are fitted at the reflector end of the boom and the coaxial cable fed through the boom to the driven elements.

Photo 4

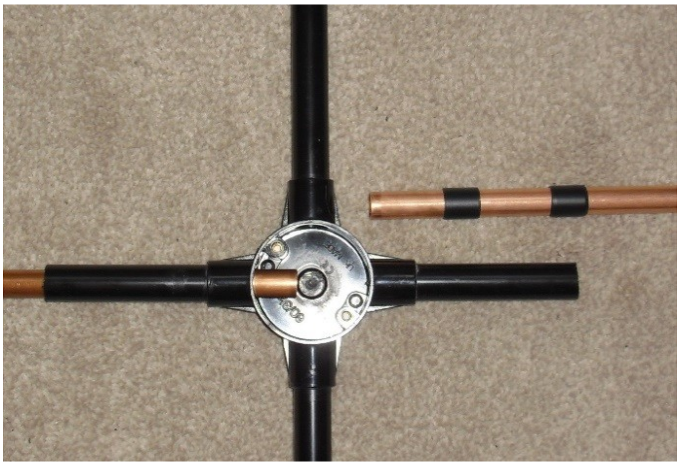

If using the conduit option "C" add two 'collars' each of 8 or 9 turns of insulating tape around the 15 mm pipe sections to form a tight fit within the conduit as shown in photo 4. Add sealant around the conduit exit points as a safeguard against water penetration.

The Director and Reflector

These are sometimes known as 'parasitic' elements because they have electrical properties but are not connected to anything, unlike the Driven elements (or Dipole) described later.

Antenna A (see photo 1) uses 16 mm mini trunking to support the Director and Reflector elements. Short lengths are screwed to the boom and the copper pipe sections simply snapped into them. The trunking lid is not needed.

Antenna B has the Director and Reflector elements secured to the wooden boom by 15 mm holes drilled through the boom section leaving a 1mm bridge. This is easier said than done unless you have a drill bit capable of drilling a clean exact size hole. So a slot 15mm wide and deep would be just as good with the added step during final fitting of bedding it in silicon sealant to ensure a tight fit and weatherproofing and then removing any surplus. The 15 mm pipe is secured by a self-tapping screw on the underside.

Photo 5

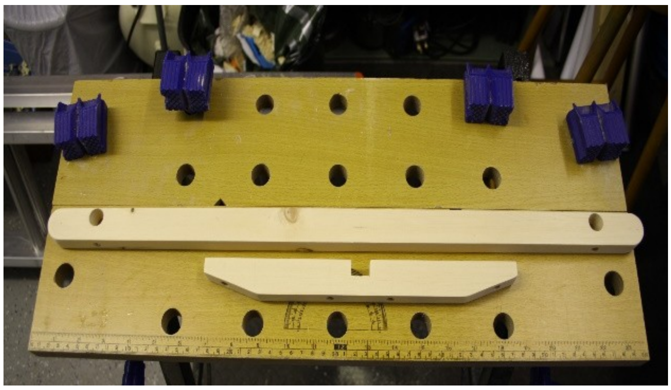

Alternatively you can use lengths of 20mm conduit, either with a junction box or fastened to a wooden boom with saddles. As with the Driven Elements, you will need to pad out the copper pipe with insulating tape to form a tight fit in the conduit.

Connecting Cable

A wide range of coaxial cables and connectors with the required impedance of 50 ohms are available, but even to experienced radio amateurs fitting the connectors is not the easiest of tasks. So unless you feel competent to buy the cable [RG58 good quality] and fit the plug, purchasing a ready-made lead with BNC connectors fitted and chopping one end off may be the most practical solution, although more expensive. Depending upon the type of receiver you use you may need an additional BNC adaptor to suit the particular type of antenna socket it is fitted with.

Connect the un-terminated end of the cable to the two driven elements by threading the cable through the cable gland into the box and pull enough through to allow comfortable working. Remove about 40 mm of the outer insulation by pressing a sharp knife around the circumference of the cable without using a “sawing” motion to avoid cutting the braid, then gently tease out the braid; a pointed tool is often an aid here, then twist the braid together to form a single wire. Strip about 15mm of insulation off the inner conductor, again avoiding a sawing action that can damage the inner conductor. Then wrap both conductors around the final connection screws using suitable washers to secure the conductors.

Ensure the screws are tight and no thin strands of braid are causing a short. If you have some silicon grease or a spot of Vaseline, apply a thin coat to the connections. **Do not use silicon sealant here as this can create corrosion problems.**

Secure the cable to the boom using plastic tie wraps or similar, making sure that you do not stress the cable at the entry to the connection box. If the cable is coming downwards to the connection box it’s a good idea to include a ‘drip-bend’ to avoid rain water running down the cable and pooling over the compression seal.

Connections to Driven Elements

Photo 6 Antenna A

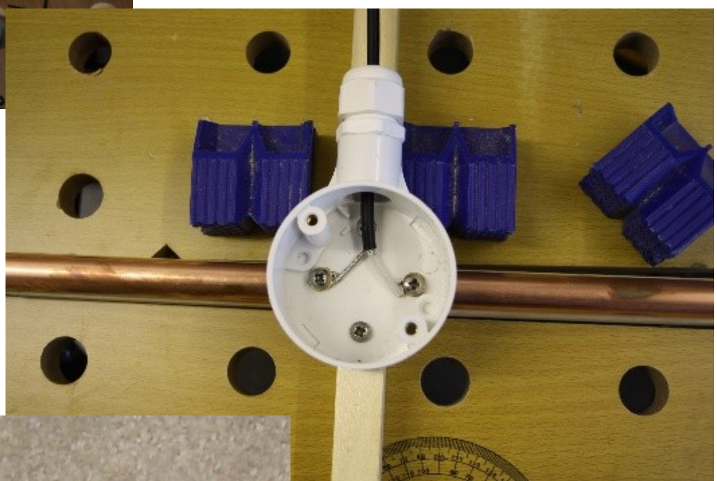

Photo 7 Antenna B

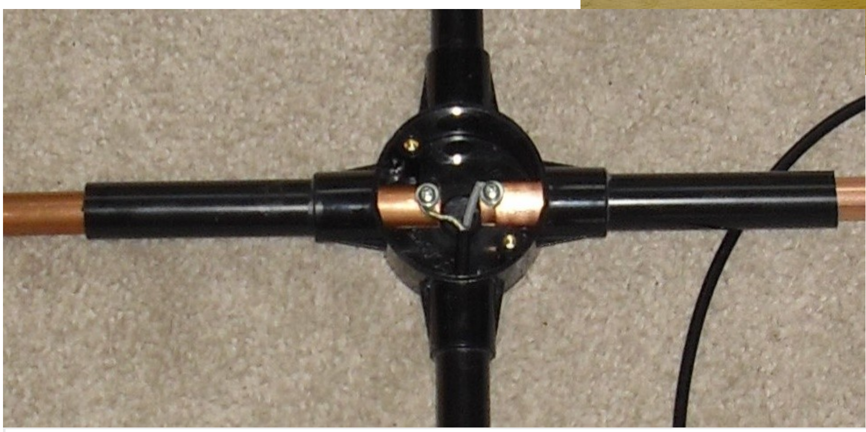

Photo 8 Antenna C

Completed antennas

Antenna A

Antenna B

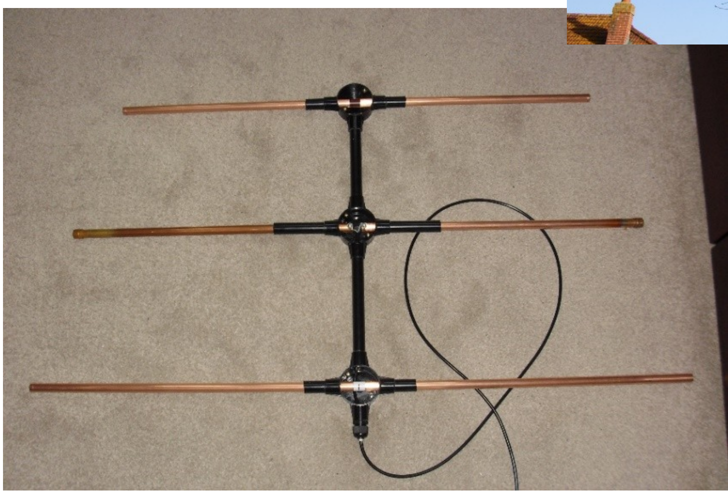

Antenna C (box covers not fitted)

Antenna Performance

The chart below compares the performance of the various options. Standing Wave Ratio, more commonly known as SWR, is a measure of how well a signal is transferred between the antenna and the receiver. A poor SWR figure (a poor 'match') will result in some of the signal being reflected backwards, rather than carrying on down the cable towards the receiver. The SWR figure is less important for a receive-only antenna than for one also used for transmission. A poor match in the latter will result in more transmitter power being reflected back to the transmitter, which reduces the effectiveness of the antenna and can cause problems for the transmitter itself. A ratio of less than 2:1 will generally be acceptable for a receive-only antenna.

Whilst the SWR figure doesn't tell you anything about how directional an antenna is, it does provide an easily measurable way of checking the operation of the antenna.

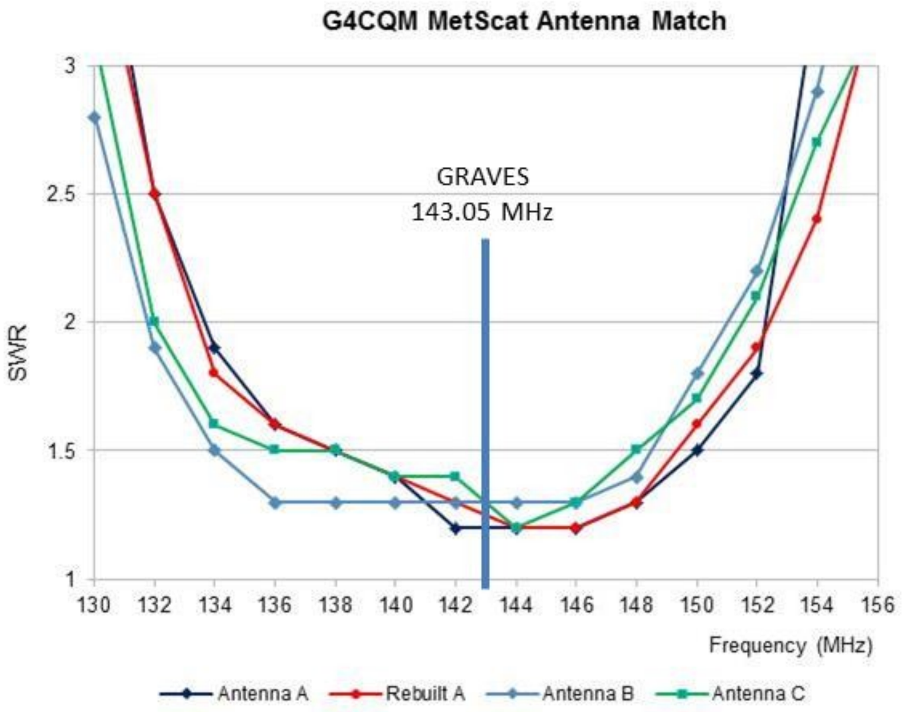

(Antenna A was measured and then rebuilt using the same elements and target spacing distances, but manufacturing error resulted in the spacings being about 5 mm too small. This has not affected the SWR figure to any real significance.)

From these figures you can see that providing the quoted dimensions are adhered to. construction techniques are very flexible.

————-